BACHELOR PAPER

Term paper submitted in partial fulfillment of the requirements for the degree of Bachelor of Science in Engineering at the University of Applied Sciences Technikum Wien - Degree Program Biomedical Engineering

Dosimetry of Ir-192 brachytherapy sources

By: Ing. Daniela Loisinger

Student Number: 1810227038

Supervisor: Ing. DI Dr. techn. Claudia Waldhäusl

Vienna, May 20, 2021

Declaration

"As author and creator of this work to hand, I confirm with my signature knowledge of the relevant copyright regulations governed by higher education acts (see Urheberrechtsgesetz /Austrian copyright law as amended as well as the Statute on Studies Act Provisions / Examination Regulations of the UAS Technikum Wien as amended).

I hereby declare that I completed the present work independently and that any ideas, whether written by others or by myself, have been fully sourced and referenced. I am aware of any consequences I may face on the part of the degree program director if there should be evidence of missing autonomy and independence or evidence of any intent to fraudulently achieve a pass mark for this work (see Statute on Studies Act Provisions / Examination Regulations of the UAS Technikum Wien as amended).

I further declare that up to this date I have not published the work to hand nor have I presented it to another examination board in the same or similar form. I affirm that the version submitted matches the version in the upload tool."

Vienna, May 20, 2021

Daniela Loisinger

Signature

Kurzfassung

In der radiologischen Therapie, im Besonderen in der Brachytherapie ist es erforderlich für jeden Patienten eine individuelle Bestrahlung durchzuführen. Für die erforderlichen Bestrahlungsberechnungen stehen Bestrahlungsplanungssysteme zur Verfügung. Diese unterliegen, aufgrund der hohen Anforderungen, speziellen Richtlinien und müssen regelmäßigen Überprüfung unterzogen werden.
Für diese Überprüfung stehen unterschiedliche Normen bereit. Diese Normen beinhalten derzeit für die Brachytherapie keine Vergleichsmessungen zwischen kalkulierten Planungswert und Bestrahlungswert, wie sie in der Teletherapie bereits verwendet werden. Um diese Vergleichsmessungen auch für die Brachytherapie umzusetzen, wird in dieser Studie überprüft, ob mit Detektoren, die bereits in der Teletherapie angewendet werden, Messungen auch im Brachybereich mit guten Ergebnissen möglich sind. Mittels dosimetrischer Messungen werden diese Daten erhoben, um die Plausibilität der berechneten Daten zu überprüfen.
Für die Versuchsreihe stehen High Dose Rate (HDR) Ir-192 Quellen zur Verfügung. Die Messungen werden mit zehn unterschiedlichen Detektoren sowie zwei Elektrometer von den Herstellern iba und PTW durchgeführt. Die Messungen erfolgen in Wasser-Phantomen. Es stehen drei unterschiedliche Phantome zur Verfügung, von denen zwei speziell für diese Versuchsreihe konstruiert und angefertigt wurden. Die erhobenen Daten werden mittels der berechneten Werte des Oncetra Brachy Planungssystems des Herstellers Nucletron/Elekta verglichen. Die Messergebnisse liefern sehr positive Ergebnisse.
Zusammengefasst lässt sich sagen, dass eine Anwendung der Detektoren auch für die Brachytherapie einsetzbar ist. Dies ermöglicht es, dass Vergleichsmessungen in der Abnahmenorm von Brachytherapie Einrichtungen mit aufgenommen werden können.

Schlagworte: Brachytherapie, Bestrahlungsplanungssystem, Ir-192, High Dose Rate (HDR), Detektoren

Abstract

In radiological therapy, especially in brachytherapy, it is necessary to carry out individual irradiation for each patient. Treatment Planning System (TPS) are available for the necessary radiation calculations. Due to the high requirements, these are subject to special guidelines and must be regularly checked.
Different standards are available for this review. These standards currently do not include comparative measurements between calculated dose and irradiation dose for brachytherapy, as they are already used in teletherapy. In order to implement these comparative measurements for brachytherapy as well, this study will examine whether measurements in the brachytherapy range are also possible with good results using detectors that are already used in teletherapy. By means of dosimetric measurements, these data will be collected in order to check the plausibility of the calculated data.
High Dose Rate (HDR) Ir-192 sources are available for the test series. The measurements are carried out with ten different detectors and two electrometers from the manufacturers iba and PTW. The measurements are carried out in water phantoms. Three different phantoms are available, two of them were specially designed and manufactured for this series of experiments. The collected data are compared with the calculated values of the Oncetra Brachy planning system from the manufacturer Nucletron/Elekta. The measurement results are very positive.
In summary, it can be said that one application of the detectors can also be used for brachytherapy. This makes it possible to include comparative measurements in the acceptance standard of brachytherapy facilities.

Keywords: Brachytherapy, Treatment Planning System (TPS), Ir-192, High Dose Rate (HDR), Detectors

Acknowledgements

Ich möchte mich besonders bei meiner Betreuerin Ing. DI Dr. techn. Claudia Waldhäusl bedanken, die es mir nicht nur ermöglichte mein Praktikum in der Klinik Donaustadt zu absolvieren. Sondern die mir auch im Zuge des Praktikums und der Verfassung der Bachelorthesis zur Seite stand. Ihre Anregungen, Wissen und Begeisterung für die Materie Brachytherapie waren ansteckend und haben einen großen Beitrag zu diesem Werk geleistet.

Des Weiteren möchte ich die Personen hier erwähnen die mich während meiner Studienzeit direkt wie indirekt unterstützt haben.

Meine Familie, die mir den Raum und die Zeit gab meinen Weg zu gehen, auch wenn die Begeisterung für mein Studium zu Beginn nicht so gegeben war. Ich weiß das ich in euren Augen dafür schon zu Alt war, ihr habt aber alle zu beginn gewusst, dass ich meinen Sturkopf durchsetzen werde und die Sache auch durch ziehe.

Meine Freunde, die mich während den Höhen und Tiefen begleitet haben und mir immer mit Rat, Tat und Meinung zur Seite standen. Ich weiß bis zum heutigen Tage nicht wie ich mich bei jedem von euch jemals erkenntlich zeigen kann.

Meine Feuerwehrkolleginnen und Feuerwehrkollegen die auf ein paar helfende Hände die letzten Jahre verzichten mussten. Wenn alles vorbei ist stehe ich wieder an eurer Seite und unterstütze euch wieder nach Leibeskräften.

Contents

1 Introduction

1.1 Problem area

In radiotherapy, to provide patients with optimal care, it is necessary to carry out extensive treatment planning. In the age of computers, medical physicists and technicians are supported by dedicated Treatment Planning System (TPS). Especially in brachytherapy, where the radiation source is positioned directly inside the body, by usage of applicators, the patient is exposed to a high radiation dose [1, p. 1], [2]. This requires precise treatment planning of the irradiation and thus places high demands on staff and equipment. To avoid errors, irradiation TPS are subjected to regular Quality Assurance (QA) tests, which are regulated by various standards. These QA tests are based only on recalculations or checks with existing data [3], [4]. Therefore it is planned to carry out QA measurements. For this purpose, different phantoms with simple geometry and different detectors will be used. By comparing the measured and calculated dose, errors in the TPS can be detected.

The problem described above gives rise to several hypotheses for the study:

- Is a regular change in quality control necessary at all?
- Are the calculations of the TPS at all comparable with measurements, as the detectors are used usually in teletherapy?
- How far do measured and planned doses differ?
- Based on the detectors available for measurements, which are the most suitable once?

In order to answer these questions, quantitative methods are used to collect data to check the plausibility of the calculated data. For this purpose, the measured data are compared with the calculated data to be able to determine the deviation. These differences is decisive. During these measurements, a guideline is to be developed on how the measurements are to be carried out. Independently of this bachelor thesis, the guideline will later be integrated into the QA. Thus, this bachelor thesis is the cornerstone for the amendment of the ÖNORM S 5296 [4].

1.2 Insight into the matter

1.2.1 Brachytherapy

The word brachytherapy (<gr.> $[\beta\rho\alpha\chi\upsilon]$ brachy, <engl.> short) means short-distance therapy. This means that a radiation source is applied inside a localised tumour. The steep dose gradient of a radiation source is used. Near the source, the dose falls very quickly due to the inverse square law ($1/r^2$). This causes an increase in radiation in the vicinity of the tumour, but the surrounding tissue or organs are spared due to the steep fall-off [5, p. 123], [6, p. 580]. The purpose of this radiation enhancement is to damage the Deoxyribonucleic acid (DNA) in the human cell nucleus by means of ionising radiation. The aim of this targeted damage is to damage the tumour cells so irreversibly that it goes into cell death or suffers permanent cell cycle arrest. Cell cycle arrest is when cells are no longer able to divide due to their damage. The cell death itself does not appear immediately, the cell is still able to proliferate for a certain time, but mostly it has lost its ability to divide indefinitely, which is equivalent to apoptosis due to the DNA damage. For targeted damage of the tumour, doses of approx. 20 - 100 Gy are necessary; it is important that the dosage is adapted to the healthy tissue. Only the dose that does not cause serious radiation consequences in the healthy tissue but still is high enough to eliminate the tumour should be administered [7, pp. 25, 35]. [8, pp. 29–30]

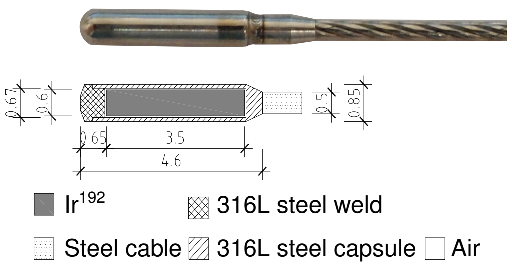

Figure 1: Structure of the Ir^{192} source with comparison to a photo of a dummy source. All dimensions are in mm (Source: modified taken from [9, p. 79]).

Various devices such as applicators, tubes and needles are available for guiding the source inside the patient. However, the core piece for successful brachytherapy is the afterloader. It contains the Ir^{192} source with the dimensions 3.5/0.6 mm (W/H) [9, p. 79]. This source is encased in a stainless steel capsule which is located at the end of a twisted steel cable. A picture with the dimensions of the source and a source cable can be seen in figure 1. The source itself is located in a safe in the afterloader. When irradiation is initiated, a dummy source first travels through the applicator. This is to check that the transfer tube and applicator are free of obstructions and of the correct length. Only then the source moves out of its safe and travels via the transfer tube to the applicator. The dummy source and the source are controlled by means of a stepper motors that can control step widths of 1 mm. It is also possible to move the source out via one of several channels. An picture of the Afterloader devices is shown in figure 2. [8, pp. 84–88]

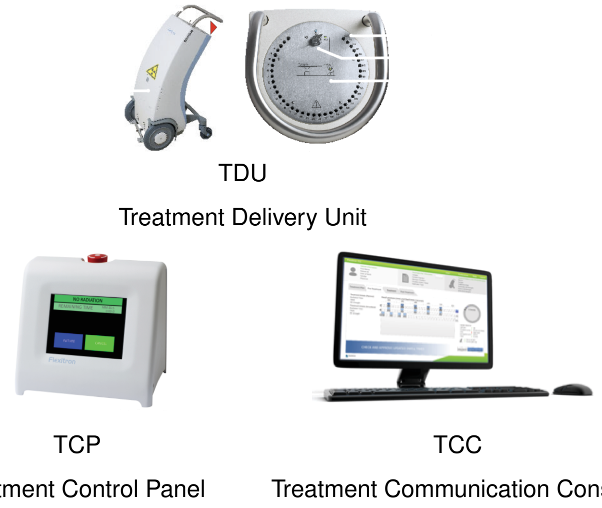

Figure 2: The Afterloader Treatment Delivery Unit (TDU) and his peripheral devices Treatment Control Panel (TCP) and Treatment Communication Console (TCC) (Source: modified taken from [10]).

1.2.2 Ir^{192} Source

In brachytherapy in particular, it is necessary to use different nuclides depending on the area of application. Whether irradiation is carried out by means of an afterloader or direct implementation in the body by means of seeds places different demands on the nuclide. For use in afterloaders, nuclides with a long half-life and high specific activity are preferred. Long half-lives allow the source to be in use for a long time, especially for nuclides that have to be produced artificially, a long usability represents a cost saving. A high activity makes it possible to produce very small-volume sources, which in turn make it possible to produce small and elastic source cables. Furthermore, it should be considered into which products the nuclide decays, as the decay products could also form radioactive substances. The most widely used isotope in brachytherapy in Europe is Ir^{192} [11]. Its half-life of 73.81 days and its high specific activity of 340.98 GBq mg^{-1} qualify it for use in afterloaders [12, p. 5]. [8, pp. 34–35]

Ir^{192} is generated from an Ir^{191} nuclide and the (n,γ) reaction [13]. In the (n,γ) reaction, a thermal neutron is captured in a reactor by the target nucleus, in this case Ir^{191}, forming a compound nucleus [14, p. 128]. By a thermal neutron Krieger et al. mentioned, that a "*neutron whose kinetic energy is of the order of the most probable thermal energy of a gas atom at room temperature*" [15, p. 203]. As a conclusion it can be said that a High Dose Rate (HDR) Ir^{192} source is created by Ir^{191} absorbing a neutron. [11]. Sources whose dose rate is higher then 12 Gy/h count as HDR sources [2].

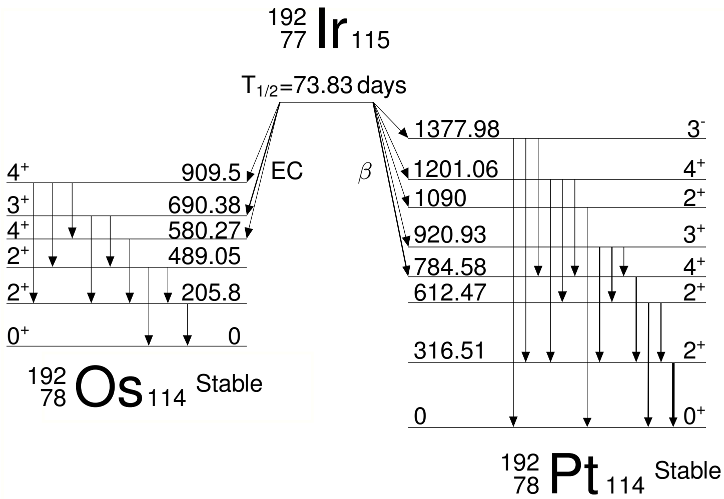

Figure 3: Decay schema of the radioisotope Ir^{192} (Source: modified taken from [16], [17]).

Ir^{192} decays by β radiation into platinum and by Electron Capture (EC) into osmium, both nuclides are stable [16]. During its decay, it emits 2.3 gamma rays per decay with an average energy of 0.355 MeV [13], [8, p. 35]. A decay schema with the exact energy levels can be seen in figure 3.

1.2.3 Treatment Planning System (TPS)

A TPS is defined in the standard Norm S 5295 as a programmable electronic system, which also includes all connected peripheral devices, that is used to simulate a radiation application to a patient. In practice, this means that calculations are made with calculation algorithms and stored databases that enable radiation planning. In addition to the special technical advances of recent years, Computed Tomography (CT) images of the patient can be fed into the TPS and thus optimise the treatment planning. Despite this progress, the formulas and data on which the calculations are based have remained largely the same. For TPS, the basis is Task Group No. 43 Report of American Association of Physicists in Medicine (AAPM). This report contains all the necessary formulae, including an explanation of them. Furthermore, for each radiation source of the different manufacturers a short description is given with a technical drawing as well as the tables with the data for the anisotropy function. The Klinik Donaustadt has an Oncentra Brachy TPS which calculates dose rate using the equation 1. [18], [9], [19]

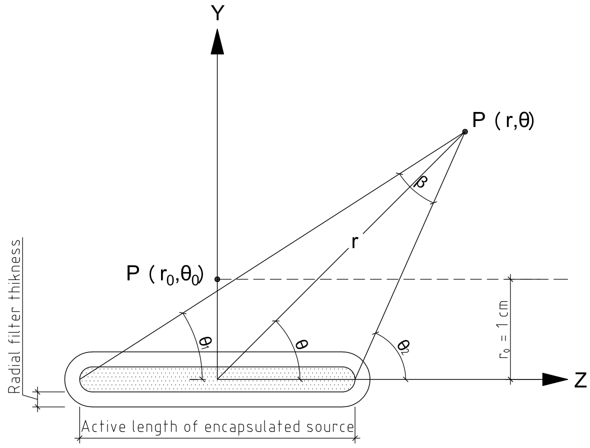

Figure 4: Geometry for the dose calculation formalism; see equation 1. $P(r,\theta)$ represent the Point-of-interest and $P(r_0,\theta_0)$ means the reference point (Source: modified taken from [11]).

$$\dot{D}(r,\theta) = S_k \Lambda \frac{G_x(r,\theta)}{G_x(r_0,\theta_0)} F(r,\theta) g_x(r) \tag{1}$$

$\dot{D}(r)...Dose\ rate\ at\ ponit\ (r,\theta)\ [cGy\, h^{-1}]$
$S_k...Air\ kerma\ strength\ [U = cGy\, h^{-1}\, cm^2]$
$\Lambda...Dose\ rate\ constant\ in\ a\ medium\ using\ air\ kerma\ strength\ normalization\ [cGy\, h^{-1}\, U^{-1}]$
$G_x(r,\theta)...Geometry\ factor\ at\ point\ (r,\theta)\ [cm^{-2}]$
$G_x(r_0,\theta_0)...Geometry\ factor\ at\ point\ (r_0,\theta_0)\ [cm^{-2}]$
$F(r,\theta)\ ...Anisotropy\ function\ at\ point\ (r,\theta)\ [\,]$
$g_x(r)...Radioal\ dose\ function\ [\,]$

The treatment planning for patients includes the determination of different volumes. The gross tumour volume is determined on the basis of image data and attention is also paid to the tumour spread area. This area most likely already contains tumour cells. Once the tumour region has been determined, the clinical target volume is defined, which includes not only the primary visible tumour but also all regions that could already contain tumour cells. In order to be able to intercept volume changes during treatment, a safety space is usually set up around the clinical target volume, this is called the planning target volume. Since tumours usually do not grow uniformly, the treatment planning must be adapted to this. This means that the planning target volume differs from the treated volume. The treatment planning also takes into account the irradiated volume, which includes all areas of the body that are unavoidably exposed to radiation due to the treatment even though they are not part of the planning target volume. [7, pp. 252–254], [6, pp. 489–490]

1.2.4 Detectors

Detectors are designed to produce a signal by physical or chemical reactions when ionising radiation is exposed. These can be divided into different groups based on the radiation effect produced [5, pp. 143–144]. Ionisation chambers use the effect of ionisation in gases for detection. Semiconductors and conductivity detectors have as main effect the ionisation in solids. Semiconductor detectors include the RAZOR$^{\text{Diode Detector}}$ and the Semiconductor detectors from the manufacture PTW. The microDiamond is a conductivity detector, all other detectors used are ionisation chambers.

The main components of an ionisation chamber are the filling gas and the electrodes. The filling gas is usually air, as it is very similar to human tissue and water. When the filling gas is irradiated with ionising radiation, electron-ion pairs are created through interactions. In order to collect the primary charges generated by the ionisation of the gas and to detect them in the measuring device, it is necessary to apply a voltage to the chamber. An image of an ionisation chamber whit the main components is shown in figure 5. [20, pp. 25–30], [5, pp. 145–148]

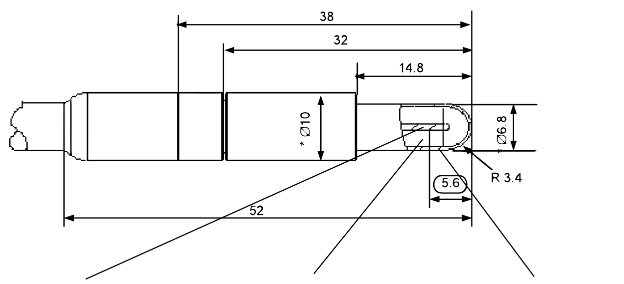

Figure 5: Cross-section view of an CC25 ionisation chamber. All dimension are in mm (Source: modified taken from [21]).

As already mentioned, the microDiamond is a conductivity detector, it consists of a synthetic single crystal diamond. Diamonds have the advantage that they are largely equivalent to soft tissue due to their low atomic number. When irradiated with ionising radiation, free electrons are produced in the conduction band, making the solid (diamond) conductive. This ionisation current can be detected by means of a measuring device. A special feature of conductivity detectors is the delayed signal detection when first irradiated. This is due to the traps (metastable intermediate level energetically between valence and conduction band) which must first be filled with electrons by means of pre-irradiation. Only when these free spaces are filled the ionisation can current flow undisturbed. [20, pp. 89–91], [5, pp. 173–175, 167]

Semiconductor detectors mostly consist of a p-i-n combination. These are diodes with a charge-free intrinsic zone. If a voltage is applied to the diode from the outside, the space-charge-free radiation-sensitive zone is formed inside. This zone acts like the volume of an ionisation chamber. [20, pp. 87–88], [5, pp. 170–172]

1.2.5 ÖNORM S 5296

The standard deals with the acceptance of TPS, whereby the acceptance takes place before the clinical commissioning. It is essential that an acceptance test must always be carried out when new radiation TPS are set up, or when essential components are changed. During the inspection, it is checked whether the TPS has been installed according to the manufacturer's instructions and is functional. Furthermore, it is checked whether the users are able to use the software without errors. In order to avoid subsequent errors, reference values are defined for the recurring weekly or monthly checks in the course of the acceptance test, to which the constancy tests must refer. [4]

2 Materials and Methods

2.1 Used Equipment and Detectors

The Klinik Donaustadt has two identical operating rooms, which two afterloaders. It is necessary to replace the sources in regular intervals. In the course of this change, the calibration data of the TPS were adapted to the new source. The calibration data of the sources used are listed in table 1 and assigned to the individual devices. The reference air kerma rate was measured by the department for quality assurance reasons. The results of the measurements chosen differences to the value of the certificate of -0.22 %, +0.38 % and +0.63 %, respectively.

Table 1: Calibration details of the three used Ir^{192} sources, specified by the production company Curium Netherlands B.V. The source in the Afterloader 1 device was change on the 22^{th} of January.

Device	Calibration Date	Calibration Time	Reference air kerma rate $\left[\frac{cGycm^2}{h}\right]$	Apparent source activity $[Ci]$	Serial number
Afterloader 1	28.10.2020	18:04	52020	12.88676	NLF01D85E5606
	07.01.2021	03:12	44810	11.10065	NLF01D85E5930
Afterloader 2	02.03.2021	15:21	50810	12.58701	NLF01D85E6191

The used phantoms were commercially available phantoms and self-made ones. The self-made phantom called needle phantom and the in-vivo phantom are jigs made of Polymethylmethycrylat (PMMA) that are immersed into a small water tank. The needle phantom is 140/180/120 mm and the in-vivo phantom is 118/120/60 mm. The water tank is 695/503/595 mm (W/H/D).

The basic structure of a measurement setup consists of the afterloader, an electrometer, a phantom, a detector and the accessories required for the individual components. Each phantom can be combined with any electrometer and measurement detector, regardless of the manufacturer. In addition, all detectors are suitable for measurements in air and water. The detectors, with the exception of the RAZOR$^{\text{Diode Detector}}$, had a calibration certificate from the companies and thus also a calibration factor for Co^{60}. The Semiconductor probes had a calibration factor measured by the department itself with Ir^{192}. The equipment for the various measurement setups is listed in table 2.

Table 2: List of the equipment and software used for the various measurement setups.

Device	Manufacturer	Model	Firmware version
Treatment Planning System (TPS)	Nucletron / Elekta	Oncentra Brachy	4.6.0
Afterloader	Nucletron / Elekta	Flexitron HDR Treatment Delivery Unit (TDU)	-
		Flexitron HDR Treatment Control Panel (TCP)	3.3.0.0103
		Flexitron HDR Treatment Communication Console (TCC)	3.3.0.0353
		Transfer tubes	-
		Application needles	-
Electrometer	iba	Dose^2	2.0.0.1
	PTW	Unidos T10001	2.40
Needle phantom	self-made	Needle phantom	-
In-vivo phantom	PTW	Multidose AL Box T16008	-
		Vividos T10018	2.40
		Multisoft	1.3
	self-made	In-vivo phantom	-
Water phantom	iba	Blue Phantom^2	-
		Water reservoir SMARTSCAN	-
	PTW	MP3 T4316	-
		MP3 Control Unit T41013	1.10
		MP3 Tandem T10011	1.10
		Water reservoir MP3 T43163	-
		Mephysto-Software	3.4
Detectors	iba	CC04	-
		CC13	-
		CC25	-
		RAZOR$^{\text{Chamber}}$	-
		RAZOR$^{\text{Nano Chamber}}$	-
		RAZOR$^{\text{Diode Detector}}$	-
	PTW	0.3 cm^3 Semiflex Chamber T31013	-
		microDiamond T60019	-
		Semiconductor detector T9112 (Rectum)	-
		Semiconductor detector T9113 (Bladder)	-

2.2 Test sequence

2.2.1 In-vivo phantom setup

For measurements with the semiconductor detectors, it was checked whether the serial numbers of the boxes matched those on the detectors. Then the two semiconductor detectors were inserted into the in-vivo phantom. One probe was placed above and one below the application needle. The application needle was placed in the intended location in the centre of the phantom. The phantom was then placed in the plastic box. The internal dimensions of the box are 372/230/267 mm (W/H/D). The box was filled with water at room temperature until there was about 50 mm of water above the phantom. The needle was connected to the afterlaoder at channel five using a transfer tube. The two detectors were connected to the Multidos AL box. The finished measurement setup is shown in figure 6.

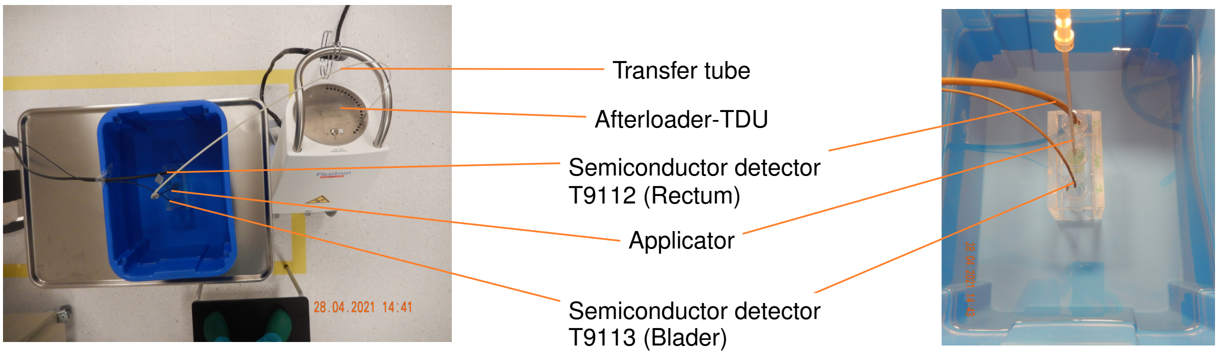

Figure 6: Measurement set-up with the in-vivo phantom.

The department has three sets of rectum and bladder probes (set A, B and C). The measurements were performed whit probe set B. Since all the probe sets were created in the Multisoft programme, only the set that was connected to the Multisoft programme had to be selected. In addition, the range was set to "High". A previously prepared irradiation plan was now started at TCC. When starting the irradiation, the measurement of the radiation dose was started simultaneously in Multisoft. After the irradiation plan was executed and the TCC indicated that the irradiation was finished, the measurement in the Multisoft software was stopped and the measured values of the probes were saved as a Portable Document Format (PDF).

2.2.2 Needle phantom setup

First a thermometer and barometer was positioned in the operating room to measure the air pressure and room temperature. These values were required for the calculation of the correction factor of the air density and temperature (p_{TP}). Depending on the electrometer used, the chamber had to be created first with the calibration certificate, if available. The instructions in the manufacturer's operating manual were followed. The exact setting options and operation of the electrometers are described in the chapters "2.2.5 Timed continuous method" and "2.2.4

Timed collection method".

The needle phantom was placed in the centre of a plastic box. All four application needles were positioned. To check whether the needles were positioned correctly, the distance between the upper edge of the phantom and the end of the needles was measured. If this was 2.9 cm, the needles were correctly positioned. The box was then filled with water at room temperature until the upper edge of the phantom was reached. The transfer tubes were now connected to the needles and these were connected to the afterloader device (channel 1 to 4). Attention was paid to the sequence (needle one to slot one etc.).

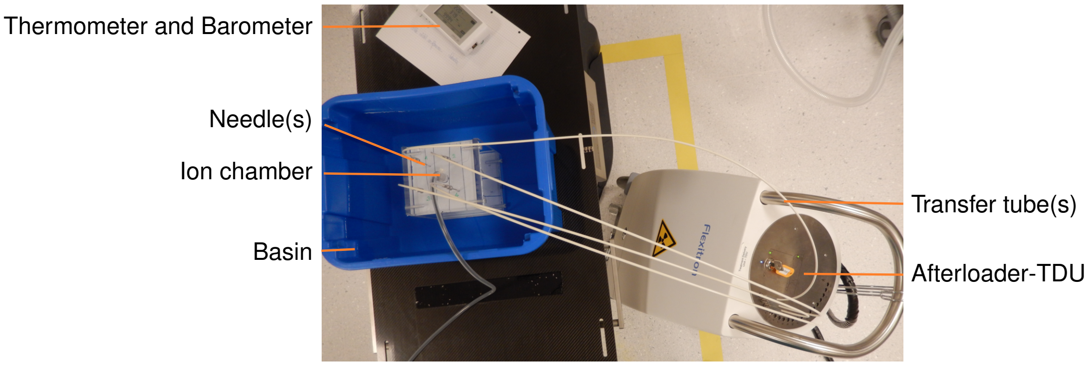

Figure 7: Measurement set-up with the 4 needle phantom.

To prepare the detector, the serial number on the detector was compared to the one of the box. Since there are several identical detectors, the risk of mismatch was minimized. The serial number was used checking the calibration certificates and the measurement documentation. The detector was connected to the already warmed-up electrometer via an extension cable and the zero adjustment was done. During the zero adjustment, the protective cap was on the measurement chamber. The detector was then inserted into the fixing device without the protective cap until the indicator mark of the detector matched with the end of the fixing device. The different detectors had different indicator marks, an example is shown in figure 8. A screw was used to fix the detector in the fixing device. The device was then inserted into the phantom. The measurement setup is shown in figure 7.

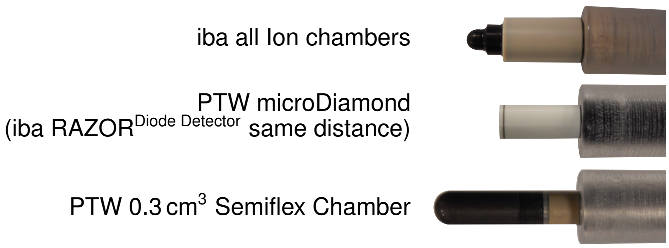

Figure 8: Indicator marks of the chambers when positioned in the fixing device.

For the "90 ° 2 needle" measurements, there were two holes for the needles on the side walls of the phantom, you can see this setup in figure 9. The phantom was placed on a flat, hard surface so that one of the side walls faced downwards with the holes. The two needles were then inserted into the holes one after the other until they were in line with the surface. The phantom was placed in the water basin in this orientation. Now the transfer tubes were connected one after the other. In order to position the detector correctly in the fixing device, the data of the existing maximum signal measurement and the position of the two needles were used. With a simple calculation, the position of the chamber could be determined and fixed in the fixing device through the screw. The detector was then inserted into the phantom. Then the chamber was connected to the electrometer and a zero adjustment was carried out. For each of the chambers, the positioning of the detector was recalculated and implemented.

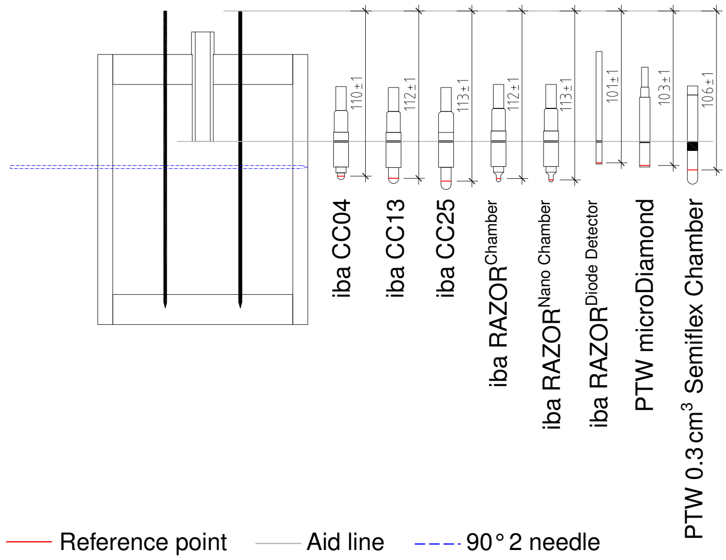

Figure 9: The needle phantom with the comparison of the ion chambers used. The detectors were always clamped in the fixture using a predefined indicator mark. Since the reference point (i.e. the geometrical center of the active volume or the effective measurement point) of the ion chambers is specified by the manufacturer, it can be determined at which extension length of the source the detectors have the highest sensitivity. Unit for the measurements is mm (Sources: influenced by [21]–[28]).

2.2.3 Water phantom setup

The basic measurement setup was the same for the two water phantoms, the Blue Phantom[2] from the company iba and MP3 from the manufacturer PTW. Since all but one of the measurements were done with the MP3 phantom, attention will be focused on this phantom.

The positioning of the needles was fixed to the water phantom in a designated and reproducible position. Figure 10 shows the setup. The needles were then inserted into the phantom. To check whether the needles were positioned correctly, the distance between the upper edge of the phantom and the end of the needles was measured. If this was 2.8 cm, each needle was placed correctly. The transfer tube was connected to the needle and to the afterloader. The water was started to be filled from the water tank into the water phantom. To do this, the water tank was connected to the phantom and the pumping system was started. During the filling process the serial number of the ion chamber was checked against that on the box.

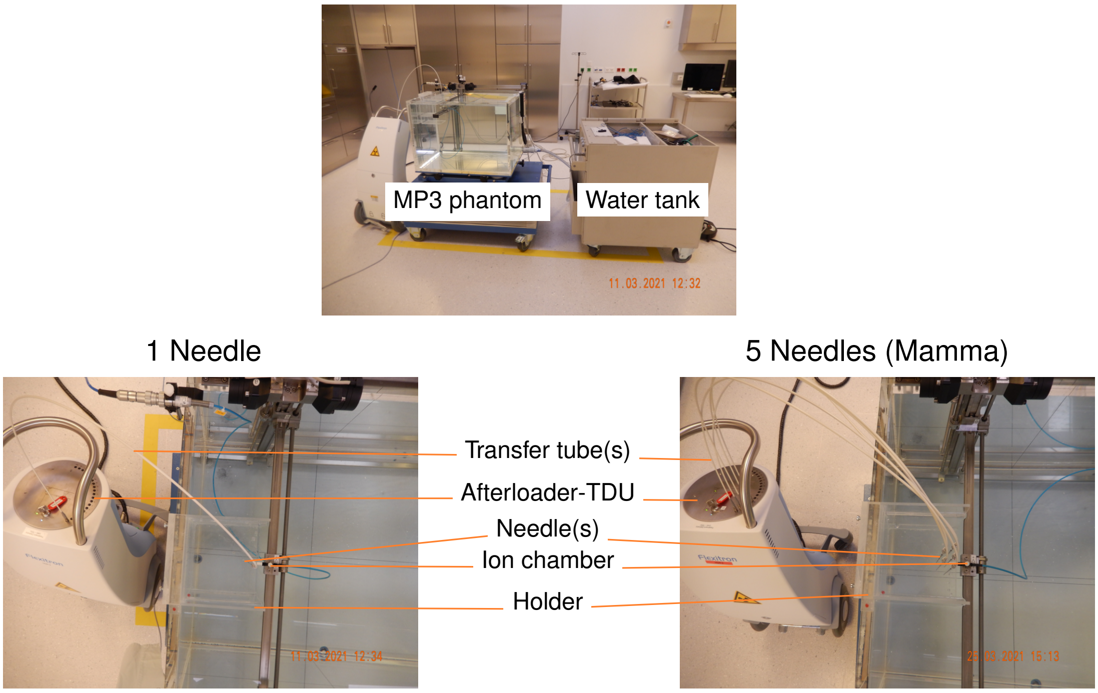

Figure 10: Measurement set-up with the Water phantom MP3 from the company PTW. In the top is the overview of the test set-up, the pictures below shows the construction in the water tank.

Next step was to insert the detector in the fixing device. The detector was inserted into the fixing device until the indicator mark of the detector matched with the end of the fixing device. An example of the different indicator marks is shown in figure 8. The microDiamond and RAZOR$^{\text{Diode Detector}}$ in the fixation was screwed in horizontal position on the undercarriage of the water phantom, the ion chambers of iba was screwed on the undercarriage in vertically position, you can see this in figure 12. The detector was connected to the electrometer via an extension cable. The electrometer, and if necessary the detector, were warmed up. After the warm-up phase, the detector was added to the electrometer library. Than a zero adjustment was performed. In addition, the barometer and thermostat, which measured air pressure and temperature, was positioned in the operating room.

After the MP3 Phantom had been filled to the wanted water level, the pump system of the water tank was turned off. Now the MP3 Control Unit was connected to the control unit of the MP3 landing gear. In addition, the Control Unit and the MP3 Tandem were connected to each other. A control cable was positioned from the control unit out into the monitoring room and connected to the laptop on which the Mephysto software was installed. Since the radiation was measured with the electrometers and ion chambers, the Mephysto software and the control unit only served to control and to change the positions of the detectors inside of the phantom.

The position of the detector could be moved in three directions by means of the undercarriage. These correspond to the usual x, y and z axes, but are named A, B and C by the manufacturer PTW. It was important for the software to set a zero point. Using this zero point, it was possible to move in all three coordinates using positive and negative values. This is shown in figure 11, which also shows the different zero positions of the individual detectors.

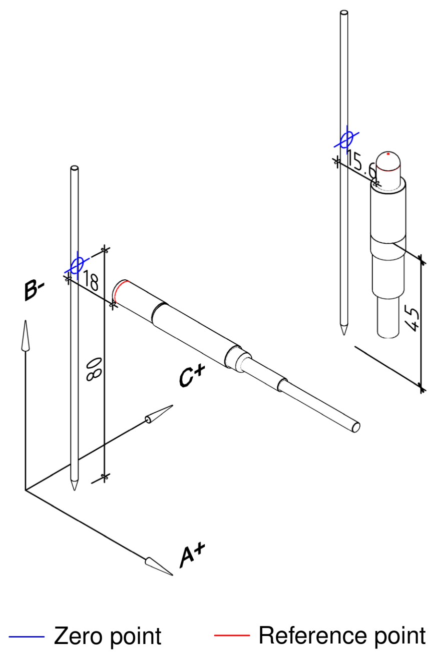

Figure 11: Coordinate axis for the Water Phantom. The absolute zero points is in the centre of the needle, the height varies depending on the ion chamber used. On the left in the picture you can see the PTW microDiamond, on the right the iba CC13 chamber at an A-coordinate of 20 mm. Due to the different reference points, the distance at A = 20 mm is also different. Movements of the detector in the A-axis enable depth dose measurements. B-axis motion make cross profile measurements possible. The C-axis was only use for 5 needles in triangular measurements. (Source: influenced by [23], [27]).

For a better understanding of the coming illustrations, it is important to explain two terms.

Absolute zero point: Centre of the radiation source and the reference point of the ion chamber when they overlap each other. A- and C-axis coordinates are both zero in this area, B-coordinate varies depending on the ion chamber. It is only a mathematical value.

Zero point: The range that can be set with the MP3 undercarriage. It is defined and stared in the control system as the zero point. All movements are carried out from there.

For defining and setting up the zero point of the microDiamond, the detector was moved to the needle until it touched the needle (A-plane). However, the needle should still be easy to move. This was to ensure that the pressure on the needle was not so high that the needle was bent. Then the detector was moved upwards from the needle tip to the centre of the needle until 80 mm was reached (B-plane). The height in the B-axis was measured using a rolling metre.

For alignment in the C-plane, it was visually checked whether the measurement chamber and needle were centred on each other (C-plane). The reference point of the ion chamber is 1 mm behind the probe head. Now, if an A-axis change of 20 mm was to be made, 18 mm was entered in the Mephysto system. This compensates for the 1 mm of the needle radius and the 1 mm of the detector to absolute zero. A picture of the zero point and the coordinates system for the microDiamond is shown in figure 11.

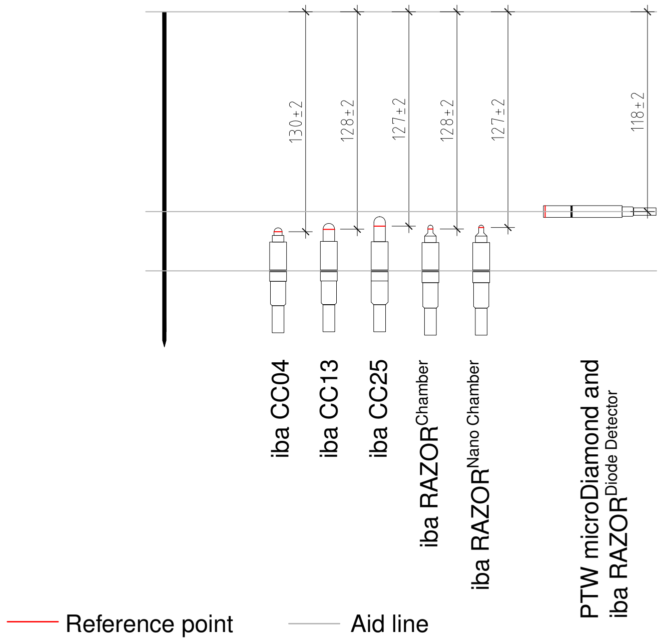

Figure 12: Representation of the detectors positioning in comparison to the needle location in the water phantom. The detectors were always clamped in the fixture using a predefined indicator mark. Since the reference point of the ion chambers is specified by the manufacturer, it can be determined at which extension length of the source the detectors have the highest sensitivity. Unit for the measurements is mm (Sources: influenced by [21]–[25], [27]).

The iba ion chambers were moved so close to the application needle that the centre of the needle and the centre of the detector were 30 mm apart (A-plane). This distance was checked using a sliding gauge. Then the ion chamber was moved in the B-axis until the indicator mark (black ring) of the detector was 45 mm away from the needle tip (B-plane). In the C-axis, the needle and detector were again only checked to see if they were aligned centrally (C-plane). This position was saved as the zero point. For the iba detectors, the reference point is located centrally in the probe head. However, since the adjusted zero point was 30 mm away from absolute zero, no mathematical corrections had to be made. The schema for the zero point for all iba ion chambers is shown in figure 11.

For position changes of the ion chamber, either the Mephysto computer control or the remote control of the phantom was used. The latter was only used to set the zero point. All coordinates in the results and tables always refer to the absolute zero point.

2.2.4 Timed collection method

This method was applicable to both electrometers of the manufacturers iba and PTW. If there were setting options that are only available on one of the devices, this will be explicitly indicated in the text.

After connecting the electrometer to the power supply and a warm up time, the ion chamber was created in the device library. This was done according to the operating instructions and all necessary data were taken from the calibration certificate of the detector, if available. The power supply for the chambers was set. For the iba detectors and the $0.3\,cm^3$ Semiflex Chamber this was 300 V and for the microDiamond 0 V.
On the PTW Unidos, by selecting the detector in the library, the user is informed that the voltage will be changed to the value stored for the ion chamber. The voltage is only changed when the start button on the Unidos is pressed, any other button aborts the process.
Then the detector was connected. With the iba electrometer, we also had to choose which channel the detector was connected to, and we always used channel one. For the selection of the range "Low", was preferred, but for some measurements it was necessary to switch to "High", otherwise the electrometer would display an error message instead of the result, because the measurement results were outside the range. With iba $Dose^2$, X were displayed on the measurement display instead of values [29]. The PTW Unidos showed the error message "OL" on the display [30]. A measuring time was now set on the device, this was in the range of 6 to 200 s. The measuring times are always given in the result tables. At the afterloader TCC the irradiation time for each position was set to the measuring time plus 15 s.

After these preparations, the actual measurement was started. The irradiation was started, if the source was at the first position and already irradiated there for 1 to 2 s, the measurement was started on the electrometer. After the specified measurement time, the device displayed the measurement result. This was noted and the result was reset. The same procedure was followed for each further position that was irradiated.

The manufacturer's instructions for the various ion chambers had to be taken into account during preparation. Some detectors required pre-irradiation or a certain minimum dose. The pre-irradiation was always carried out before beginning of the measurement recordings by simply moving the source to a certain position and irradiating there for several minutes. In order to check whether the required dose had been reached (the microDiamond requires e.g. 5 Gy), measurements were taken. The irradiation dose was adjusted so that it never fell below the dose required that some of the detectors needed.

2.2.5 Timed continuous method

This method is again applicable to both electrometer models, if settings are only applicable to one model, this will be explicitly stated in the text.
At the beginning, the electrometer was connected to the power supply and the warm-up of the device was started. The ion chamber was then created in the library if it was not already present. If it was available, it was simply selected. Then the detector was connected to the electrometer.
By selecting the desired measurement detector in the library, one was asked on the Unidos whether one now wanted to change the voltage to the stored value, with the Start button this process had to be confirmed.
On the iba, the desired voltage was selected manually in the "Bias" menu and it could be read on the display whether this was also achieved. In addition, the slot to which the ion chamber was connected had to be selected for this device. Only channel one was used for the measurements.
Next, the range was set to "Low". The range was set to "High" only when needed. The measurement time was set to "continuous", which allowed an infinitely long measurement.

After preparing the measurement chamber and the electrometer, the programming of the irradiation plan was started or sent from the TPS to the TCC. First a test cable run was carried out by the afterloader, after completion of this test cable run, a click sound indicated that the test cable had arrived back in zero position. With this sound, the start button on the electrometer was pressed and the measurement started. Then the active source moved from the safe to the programmed position. After the irradiation schedule was completed and the source was returned to the safe. The electrometer was checked for a few seconds to see if the measurement result still changed. First, if the value remained stable, it was noted.

The same procedure was used for irradiation with several needles. Since a separate test cable run was always carried out for each needle, there was enough time to note the measurement result during this pause of irradiation. It should be noted here that the time on the electrometer continued to run permanently during the entire measurement. The measurement result was not reset at any time. The summed value was always taken. Only after all needles and positions had been irradiated and the TCC indicated that the irradiation was finished, the measurement was stopped on the electrometer.

2.2.6 Radiation and measurement procedure

Due to its technical construction and the extensive possibilities, the TDU is able to move the Ir^{192} source at any position inside the needle. Due to this fact, two possible radiation applications were used during the test series. On the one hand, the "point-source", where the source was moved to a predefined position and remained at this position during the entire measurement process. On the other hand, the "activ length", where the source moved a defined distance inside the needle according to an treatment plan programmed in advance in the TCC. For both applications, it was necessary to define the positions in the needle and the dwell times in the positions. The needle itself has a length of 190 mm, in TCC it is possible to move the source the positions in millimetre steps.

"Point-source" irradiation was used in the needle phantom and water phantom for the measurements dose linearity of point-source, comperative measurments of 2 and 4 needles, point-source - Depth dose, Point-source - cross profile and dependance on water heights. "Active length" was applied in all three phantoms used and in the measurements not listed above. The exception was the comparative measurements of all detectors an one day, where both point-source and "active length" were used.

Another additional adjustment application is the water phantom. In contrast to the in-vivo and needle phantom, where the chambers are fixed rigidly in the phantom, the chassis of the phantom can be driven in three directions. The exact designation of the axes and the setting options have already been explained in detail in the chapter "2.2.3 Water phantom setup". For the measurements, driving with the chamber in three coordinates also resulted in three measurement possibilities. For the depth dose, the detector was moved away from the needle in the A-axis. The distance between the chamber and the needle could be increased millimetre by millimetre. In the cross profile, the detector was brought to a certain distance from the A-axis (= equlaterial distance). Then the needle was moved along the B-axis by means of the chamber. Since millimetre positioning was also possible here, the entire length of the needle could be traversed. With the five needles in triangular configuration, the chamber was moved to an equlateral distance of 18 mm. Then the chamber was moved step by step in the C-direction so that the distance to the needle was increased further. The total of five setting options made the high number of different measurement methods possible.

3 Results

To calculate the correction factor for the air the equation 2 was used; this is specified in the standard Norm S 5234-2. There are two notations for the correction factor p_{TP} [31] and the k_P [32], throughout the document the notation of standard S 5234-2 has been used.
For all the presented tables "deviation" (equation 3) and "deviation of normalised data" (equation 5) were calculated. The "derivation" is the difference between measured dose and the calculated dose. For calculating the so called "deviation of normalised data" both, the measured and the calculated doses, were normalised to the dose in a specific point (equation 4) and then compared. This specific point dependent on the individual measurements, see table 3.

Table 3: Listing of the specific dose points for normalisation.

Treatment	Normalised to (Point X)	
	A-axis	B-axis
Needle phantom		
Dose linearity of point-source	Time per position 50 s	
Water phantom		
Dose linearity of point-source	Time per position 60 s	
Point-source - depth dose	20 mm	-
Point-source - cross profile	e.g. 10, 15, 20, 30 mm	0 mm
Active length - depth dose	20 mm	-
Active length - cross profile	e.g. 10, 20, 30 mm	0 mm
5 needles in triangular configuration	20 mm	-

$$p_{TP} = \frac{p_0}{p} \cdot \frac{T}{T_0} \tag{2}$$

$p_{TP} ... Air\ density\ correction\ factor\ [\,]$
$p_0 ... Reference\ air\ pressure\ 1013\,hPa\ [hPa]$
$p ... Air\ pressure\ [hPa]$
$T ... Temperature\ [K]$
$T_0 ... Reference\ temperature\ 293.2\,K\ [K]$

$$Deviation\,[\%] = \left(\frac{Measured\ dose}{Calculated\ dose} \cdot 100\right) - 100 \tag{3}$$

$$Normalised\ calculated/measured\ dose\,[\%] = \frac{Value \cdot 100}{Value\ at\ point\ X} \tag{4}$$

$$Deviation\ of\ normalised\ data\,[\%] = Normalised\ calculated\ dose - Normalised\ mesured\ dose \tag{5}$$

3.1 Findings of the in-vivo phantom measurements

The measurements with the semiconductor detectors showed that the Rectum probe (R)3 and Bladder probe (B) samples with 4 % in the mean value showed the lowest deviation from the calculated dose. R5 showed the highest deviation with mean 13.6 %, from the individual measurements shown in table 4 it can be seen that this high deviation applied to all Measurement Series (MS).

Table 4: Difference between the calculation of the TPS and the measurements.

Setup	R1 [%]	R2 [%]	R3 [%]	R4 [%]	R5 [%]	B [%]
MS 1	4.4	8.2	8.1	8.2	13.6	-1.2
MS 2	6.0	10.2	7.6	8.7	15.6	-2.9
MS 3	10.1	9.4	2.1	6.6	15.4	-4.6
MS 4	3.5	4.0	-0.2	1.2	9.9	-5.1
Mean	6.0	8.0	**4.4**	6.2	**13.6**	**-3.5**
SD	2.5	2.4	3.5	3.0	2.3	1.5

When comparing the linearity, the figure 13 shows that all detectors had linearity at 2 Gy. The R3 and B samples were so congruent that they covered each other in the graph. It was also observed that fluctuations, as they occurred at 0.5 Gy, were present in all probes, whereby the R5 showed a larger drop here.

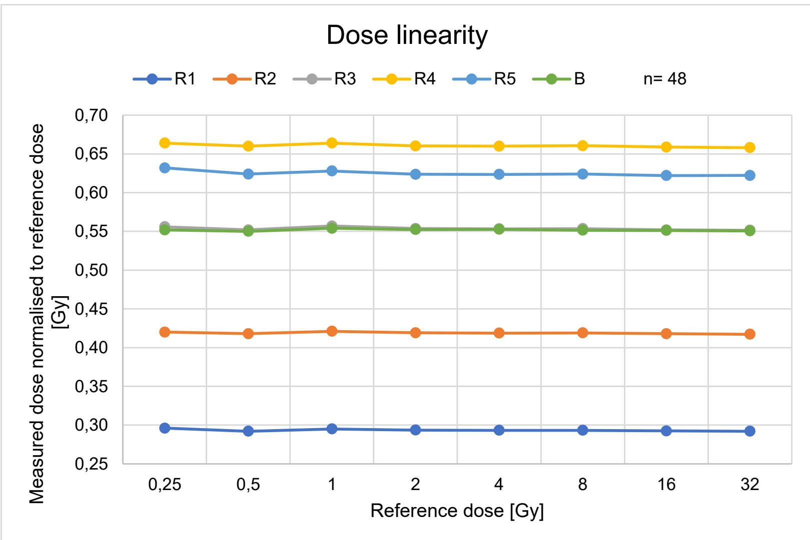

Figure 13: Diagram of the linearity by different doses from the semiconductor detectors. Eight applications were made for the rectal probe and 40 applications was made for the bladder probe. The measured values were normalised to 1 Gy. The abbreviation means Rectum probe (R) and Bladder probe (B).

3.2 Findings of the needle phantom measurements

The following graphs are used to compare the different chambers. The individual data for each detector are presented in tables, where the results for each detector are listed. The value of the max. signal calculated length in the tables was taken from figure 9. Exemplary for some measurements the detailed data are attached to the appendix.

3.2.1 Dose linearity of "point-source" irradiation

The detectors shown in the figure 14 a linear behaviour from 100 s onwards. Between 40 and 100 s there was a continuous slight decrease, before that the highest fluctuation occurred. The detectors all showed the same behaviour. Figure 15 shows, that the linearity was given for all detectors except the microDiamond from the beginning of the measurement. The microDiamond shows a slight decrease in a range from 10 to 50 s.

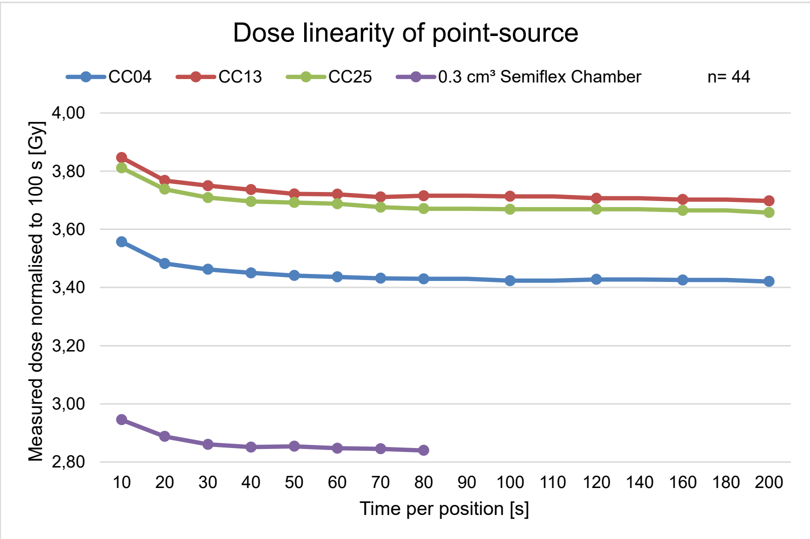

Figure 14: Diagram showing the linearity of different radiation times from all used detectors. The point dose was set for every detector individual and was placed at his max. signal high.

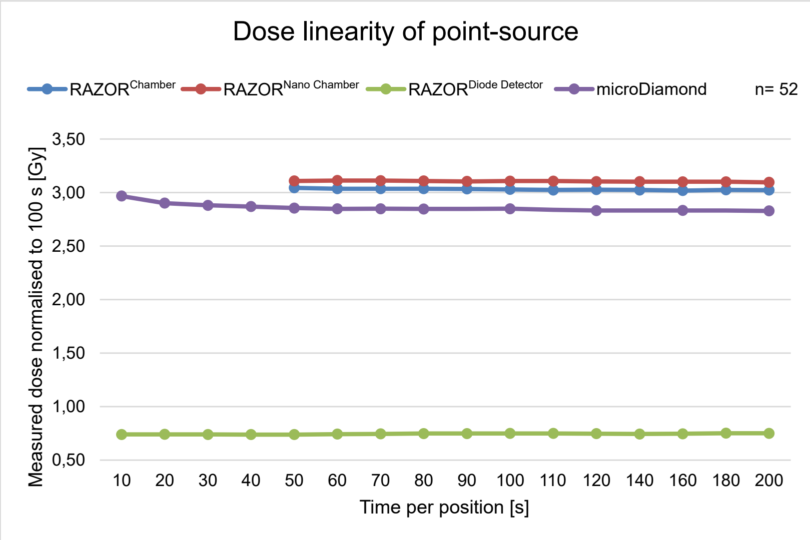

Figure 15: Diagram showing the linear of different radiation times for all used detectors. The point dose was set for every detector individual and was placed at his max. signal high.

3.2.2 Different "active lengths" irradiation

The irradiation of different lengths showed that the detectors CC04, CC25, RAZOR$^{\text{Diode Detector}}$ and microDiamond had a highest deviation of $\pm$1 %. The 0.3 cm^3 Semiflex Chamber showed a barely noticeable smaller variation of -1.5 %. The detectors CC13 and RAZOR$^{\text{Chamber}}$ had a variation of $\pm$3 %. With -6 % the RAZOR$^{\text{Nano Chamber}}$ had the highest difference to the TPS. From the figure 16 and 17 it could be seen that an increase of the irradiation length achieved a better agreement to the TPS. The improvement was different for each detector.

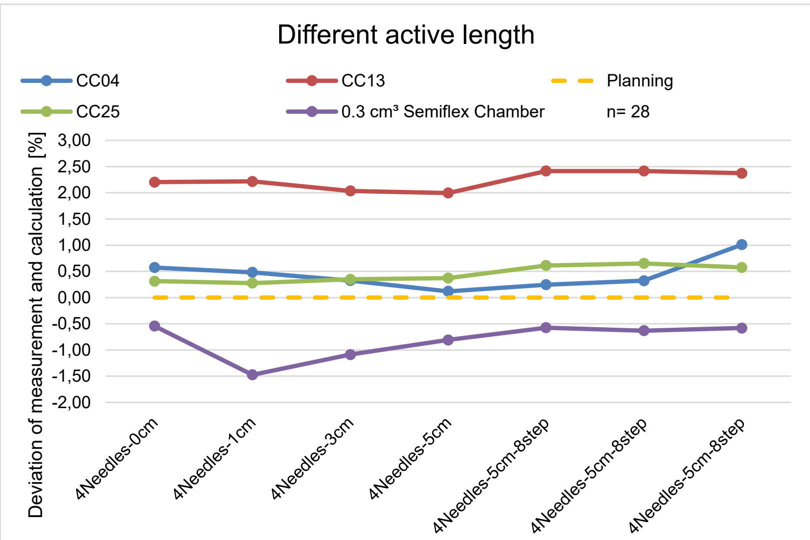

Figure 16: Diagram showing the deviations between calculated dose by the TPS (0 %) and measured for the CC's and the 0.3 cm^3 Semiflex Chamber. The point dose (4Needles-0cm) was set for detector individually and was placed at the max. signal high. The last three values (4Needles-5cm-8step) were the same.

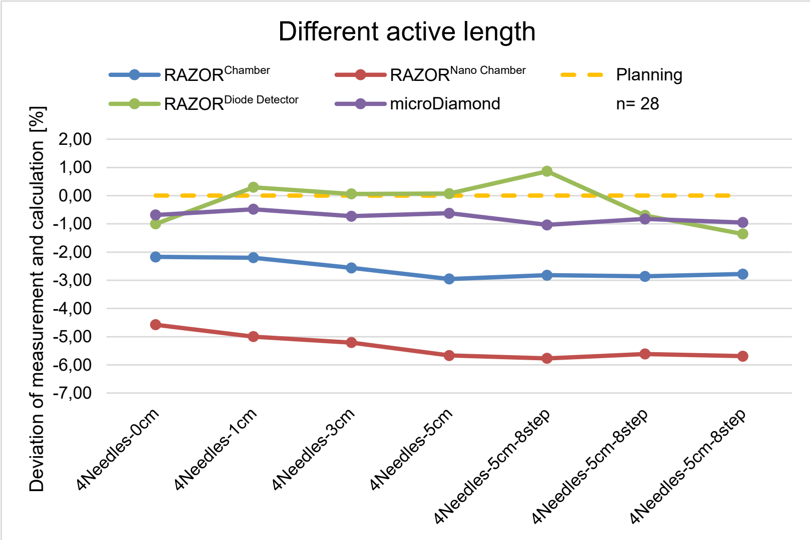

Figure 17: Diagram showing the deviations between calculated dose by the TPS (0 %) and measured doses for the RAZOR's and the microDiamond detector. The point dose (4Needles-0cm) was set for every detector individual and was placed at his max. Signal high. The last three values (4Needles-5cm-8step) were the same.

3.2.3 Comperative measurements of all detectors an one day irradiation

In the direct comparison of all detectors for "point irradiation" (figure 18) and "active length" (figure 19), all detectors showed the same behaviour. The exception is RAZOR$^{\text{Diode Detector}}$ which showed a higher deviation from the treatment planning at the 5 cm "active length". The detectors RAZOR$^{\text{Chamber}}$ and RAZOR$^{\text{Nano Chamber}}$ showed the highest difference to the calculated dose for both measurement variants.

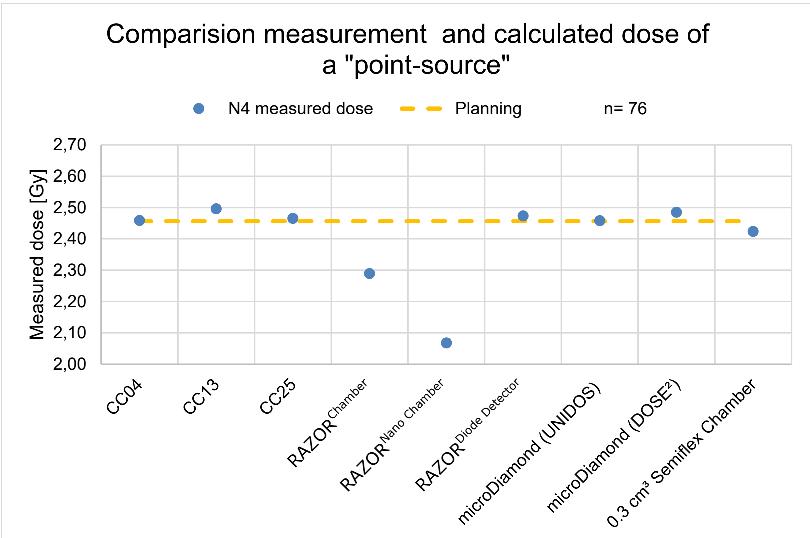

Figure 18: Diagram showing the deviations between calculated dose by the TPS and measured doses of a "point source" for the different detectors. The abbreviation mean Needle number (N).

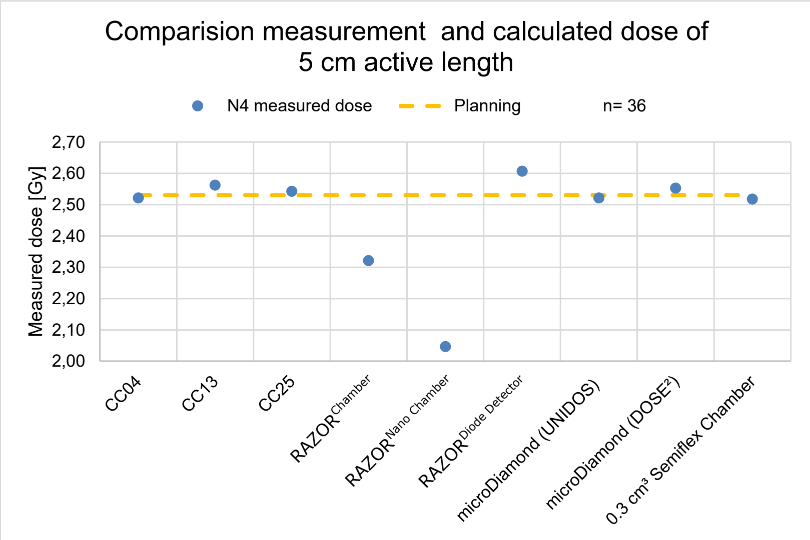

Figure 19: Diagram showing the deviations between calculated dose by the TPS and measured doses for the different detectors. The abbreviation mean Needle number (N).

3.2.4 Comperative of 2 and 4 needle irradiation

The direct comparison of the different measurement methods with 2 and 4 needles for the CC04 and CC25 showed the best agreement for measurement one and two. In figure 20 it could be seen that the CC13 always has an 1 % offset.

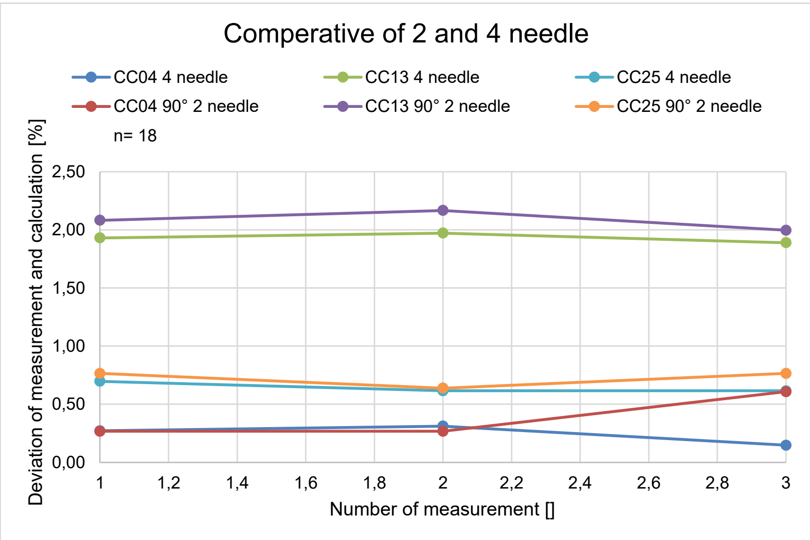

Figure 20: Diagram showing the deviations between the two possibilities using from the needle phantom.

3.2.5 Overview of all detectors

The CC04 (table 5) showed the smallest deviation between calculations of the treatment planning and the measurements for a "point-source". The dose linearity of "point-source" showed with mean 5.93 % the highest deviation for all measurements made with the CC04. Here it must be noted that the deviation of normalised data for this measurement was mean 0.24 %.

Table 5: Summary of all results for the measurements with the CC04 in the needle phantom.

<table>
<tr><td colspan="4">CC04</td></tr>
<tr><td>Treatment</td><td>Parameter</td><td>Length measured
$[mm]$</td><td>Length calculated (from figure)
$[mm]$</td></tr>
<tr><td>Distance for the max. Signal</td><td></td><td>1110 $\pm$ 1</td><td>1110 $\pm$ 1</td></tr>
<tr><td colspan="2"></td><td>Deviation
$[\%]$</td><td>Deviation of normalised data
$[\%]$</td></tr>
<tr><td rowspan="4">Dose linearity of point-source</td><td>Mean</td><td>5.93</td><td>-0.24</td></tr>
<tr><td>SD</td><td>1.13</td><td>1.07</td></tr>
<tr><td>Min.</td><td>5.06</td><td>-3.38</td></tr>
<tr><td>Max.</td><td>9.25</td><td>0.59</td></tr>
<tr><td rowspan="4">Different active lengths</td><td>Mean</td><td>0.44</td><td rowspan="4"></td></tr>
<tr><td>SD</td><td>0.27</td></tr>
<tr><td>Min.</td><td>0.12</td></tr>
<tr><td>Max.</td><td>1.01</td></tr>
<tr><td rowspan="2">Comparative measurements of all detectors an one day</td><td>Point-source</td><td>0.11</td><td rowspan="2"></td></tr>
<tr><td>Active length</td><td>-0.35</td></tr>
<tr><td colspan="2"></td><td>Deviation 4 needle
$[\%]$</td><td>Deviation Phantom 90° 2 needle
$[\%]$</td></tr>
<tr><td rowspan="4">Comparative of 2 and 4 needle</td><td>Mean</td><td>0.24</td><td>0.38</td></tr>
<tr><td>SD</td><td>0.07</td><td>0.16</td></tr>
<tr><td>Min.</td><td>0.15</td><td>0.27</td></tr>
<tr><td>Max.</td><td>0.31</td><td>0.61</td></tr>
</table>

The CC13 (table 6) detector showed the lowest deviation in the comparative measurements with the "active-length". When comparing the measurement results it can be seen that with mean 2.43 % the Dose linearity of "point-source" had the highest deviation between measured and calculated dose. The deviation of normalised data for this measurement was mean 0.29 %.

Table 6: Summary of all results for the measurements with the CC13 in the needle phantom.

CC13			
Treatment	Parameter	Length measured $[mm]$	Length calculated (from figure) $[mm]$
Distance for the max. Signal		1111 ± 1	1112 ± 1
		Deviation $[\%]$	Deviation of normalised data $[\%]$
Dose linearity of point-source	Mean	**2.43**	-0.29
	SD	1.09	1.06
	Min.	1.47	-3.37
	Max.	5.57	0.64
Different active lengths	Mean	2.24	
	SD	0.16	
	Min.	2.00	
	Max.	2.42	
Comparative measurements of all detectors an one day	Point-source	1.62	
	Active length	**1.26**	
		Deviation 4 needle $[\%]$	Deviation Phantom 90° 2 needle $[\%]$
Comparative of 2 and 4 needle	Mean	1.93	2.08
	SD	0.03	0.07
	Min.	1.89	2.00
	Max.	1.97	2.17

The comparison of all the measurement results for the CC25 (table 7) chamber showed that the comparative measurements with "point-source" had the smallest deviation. Again, the dose linearity of "point-source" showed the largest difference to the calculated dose.

Table 7: Summary of all results for the measurements with the CC25 in the needle phantom.

CC25			
Treatment	Parameter	Length measured $[mm]$	Length calculated (from figure) $[mm]$
Distance for the max. Signal		1113 $\pm$ 1	1113 $\pm$ 1
		Deviation $[\%]$	Deviation of normalised data $[\%]$
Dose linearity of point-source	Mean	**1.40**	-0.08
	SD	1.13	1.11
	Min.	0.38	-3.23
	Max.	4.59	0.93
Different active lengths	Mean	0.45	
	SD	0.15	
	Min.	0.28	
	Max.	0.65	
Comparative measurements of all detectors an one day	Point-source	**0.38**	
	Active length	0.49	
		Deviation 4 needle $[\%]$	Deviation Phantom 90° 2 needle $[\%]$
Comparative of 2 and 4 needle	Mean	0.64	0.72
	SD	0.04	0.06
	Min.	0.62	0.64
	Max.	0.70	0.77

The evaluation for the RAZOR$^{\text{Chamber}}$ (table 8) showed that the dose linearity of "point-source" had the lowest real deviation from design compared to the other measurements for this chamber. With mean 8.26 % the comparative measurements with "active length" had the highest difference.

The RAZOR$^{\text{Nano Chamber}}$ (table 9) showed with mean 19.14 % deviation for the comparative measurements with "active length", the highest achieved deviation between measured and calculated dose of all detectors used. The dose linearity of "point-source" corresponded with deviation between measured and calculated dose of mean 3.72 % to the measurements with the lowest deviation for this chamber.

Table 8: Summary of all results for the measurements with the RAZOR^{Chamber} in the needle phantom.

RAZOR^{Chamber}			
Treatment	Parameter	Length measured $[mm]$	Length calculated (from figure) $[mm]$
Distance for the max. Signal		1112 $\pm$ 1	1112 $\pm$ 1
		Deviation $[\%]$	Deviation of normalised data $[\%]$
Dose linearity of point-source	Mean	**-0.61**	0.48
	SD	0.23	0.23
	Min.	-0.97	0.00
	Max.	-0.13	0.84
Different active lengths	Mean	-2.62	
	SD	0.30	
	Min.	-2.96	
	Max.	-2.17	
Comparative measurements of all detectors an one day	Point-source	-6.79	
	Active length	**-8.26**	

Table 9: Summary of all results for the measurements with the RAZOR$^{Nano\ Chamber}$ in the needle phantom.

RAZOR$^{Nano\ Chamber}$			
Treatment	Parameter	Length measured $[mm]$	Length calculated (from figure) $[mm]$
Distance for the max. Signal		1113 $\pm$ 1	1113 $\pm$ 1
		Deviation $[\%]$	Deviation of normalised data $[\%]$
Dose linearity of point-source	Mean	**-3.72**	0.12
	SD	0.15	0.16
	Min.	-4.03	-0.11
	Max.	-3.50	0.44
Different active lengths	Mean	-5.36	
	SD	0.41	
	Min.	-5.77	
	Max.	-4.58	
Comparative measurements of all detectors an one day	Point-source	-15.81	
	Active length	**-19.14**	

The explanation of the following two tables is given on the next page 28.

Table 10: Summary of all results for the measurements with the RAZOR$^{\text{Diode Detector}}$ in the needle phantom.

RAZOR$^{\text{Diode Detector}}$			
Treatment	Parameter	Length measured $[mm]$	Length calculated (from figure) $[mm]$
Distance for the max. Signal		1104 $\pm$ 1	1101 $\pm$ 1
		Deviation $[\%]$	Deviation of normalised data $[\%]$
Dose linearity of point-source	Mean	-0.32	-0.84
	SD	0.58	0.59
	Min.	-1.16	-1.68
	Max.	0.51	0.01
Different active lengths	Mean	**-0.25**	
	SD	0.73	
	Min.	-1.36	
	Max.	0.86	
Comparative measurements of all detectors an one day	Point-source	0.71	
	Active length	**3.03**	

Table 11: Summary of all results for the measurements with the 0.3 cm^3 Semiflex Chamber in the needle phantom.

0.3 cm^3 Semiflex Chamber			
Treatment	Parameter	Length measured $[mm]$	Length calculated (from figure) $[mm]$
Distance for the max. Signal		1107 $\pm$ 1	1106 $\pm$ 1
		Deviation $[\%]$	Deviation of normalised data $[\%]$
Dose linearity of point-source	Mean	**0.40**	-0.44
	SD	1.15	1.15
	Min.	-0.53	-3.20
	Max.	3.16	0.49
Different active lengths	Mean	-0.81	
	SD	0.32	
	Min.	-1.47	
	Max.	-0.54	
Comparative measurements of all detectors an one day	Point-source	**-1.31**	
	Active length	-0.47	

In the treatment of different "active lengths", the RAZOR Diode Detector (table 10) reached the lowest deviation of all detectors with mean 0.25 %. The evaluation further showed that the comparative measurements by "active length" showed the highest deviation. The measurement of the max. signal had a difference of 3 mm when comparing measurements and the drawing.

The Semiflex Chamber (table 11) had the smallest deviation to the calculated dose with mean 0.40 % for the dose linearity of "point-source", compared to the other treatments. However the highest deviation between measured and calculated dose of mean 1.31 % for the comparative measurement with "point-source".

The microDiamond (table 12) had the lowest deviation of all chambers with mean 0.09 % for comparative measurements with "point-source" by using the Unidos electrometer. The highest difference to the treatment planning had the comparative measurements at "point-source" with the Dose^2.

Table 12: Summary of all results for the measurements with the microDiamond in the needle phantom.

microDiamond			
Treatment	Parameter	Length measured $[mm]$	Length calculated (from figure) $[mm]$
Distance for the max. Signal		1104 $\pm$ 1	1103 $\pm$ 1
		Deviation $[\%]$	Deviation of normalised data $[\%]$
Dose linearity of point-source	Mean	0.31	-0.27
	SD	1.31	1.31
	Min.	-0.92	-3.94
	Max.	3.97	0.95
Different active lengths	Mean	-0.76	
	SD	0.18	
	Min.	-1.04	
	Max.	-0.48	
Comparative measurements of all detectors an one day	Point-source (Unidos)	**0.09**	
	Active length (Unidos)	-0.35	
	Point-source (Dose^2)	**1.19**	
	Active length (Dose^2)	0.90	

3.3 Findings of the water phantom measurements

The following graphs are used to compare the different chambers. The individual data for each detector are presented in tables, where the results for each detector are listed. The value of the max. signal calculated length in the tables was taken from figure 12. Exemplary for some measurements the detailed data are attached to the appendix.

3.3.1 Dose linearity of "point-source" irradiation

Figure 21 showed that all detectors had a linear behaviour during this measurement. But there were three distinctive spots. In the case of the RAZOR^{Chamber}, a drop occurred at 160 s, which then returned to a linear pattern. The CC25 dropped continuously from 10 to 30 s continuously before it showed linearity. The RAZOR$^{Nano\ Chamber}$ exhibited a short deviation of linearity in the range of 20 s.

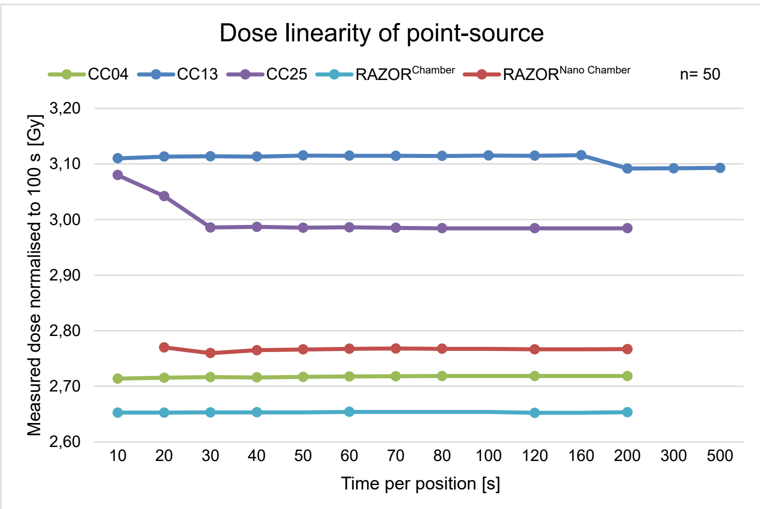

Figure 21: Diagram showing the linearity of different radiation times from all used detectors. The point dose was set for every detector individual and was placed at his max. signal high. The measurement was normalised at 100 s.

3.3.2 "Point-source" - depth dose irradiation

For the "point-source" depth dose, all chambers showed a high level of agreement with the treatment planning, as shown in figure 22. Only the values at 15 mm show a higher variation with CC25 showing the highest difference.

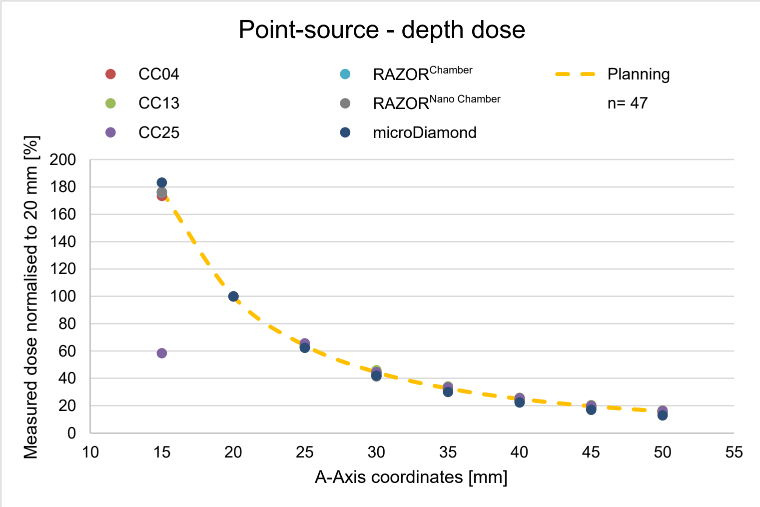

Figure 22: Diagram showing the deviations between calculated dose by the TPS and measured doses for the different detectors. The different A-axis coordinates represent the depth dose. The point dose was set for every detector individual and was placed at his max. Signal high. The measurement was normalised at 20 mm.

3.3.3 "Point-source" - cross profile irradiation

The measurements of the microDiamond and the CC25 chamber showed in figures 23 and 25 that with increasing distance of the A-axis the percentage deviation from the calculated to expected measurement result decreased more and more. The highest deviation was always in the range of 0 mm of the A-axis. The CC13 showed in its figure 24 that the distance of the A-axis caused a not so large change of the treatment planning difference. Whereby the positive deflection at 20 mm was the best match with the calculated dose.

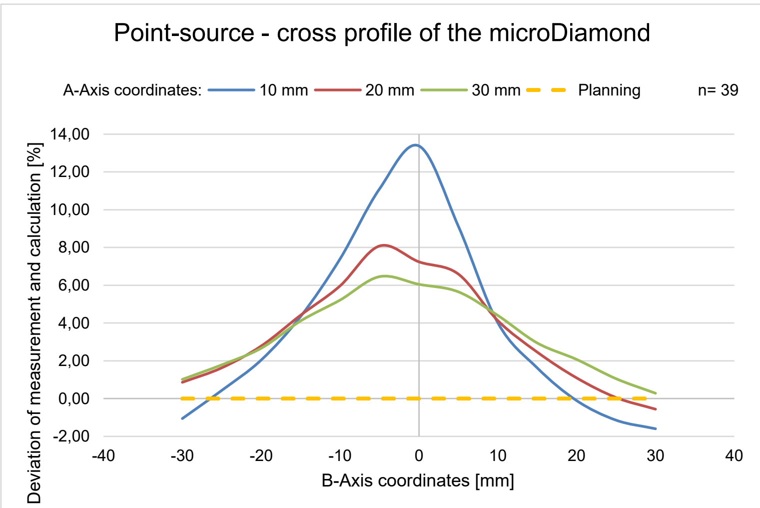

Figure 23: Diagram showing the deviation between the different Axis-coordinates A and B for the micro-Diamond. The different A-axis coordinates represent the depth dose. The B-axis represent the variation of the detector in the cross profile. The point dose was set at his max. Signal high.

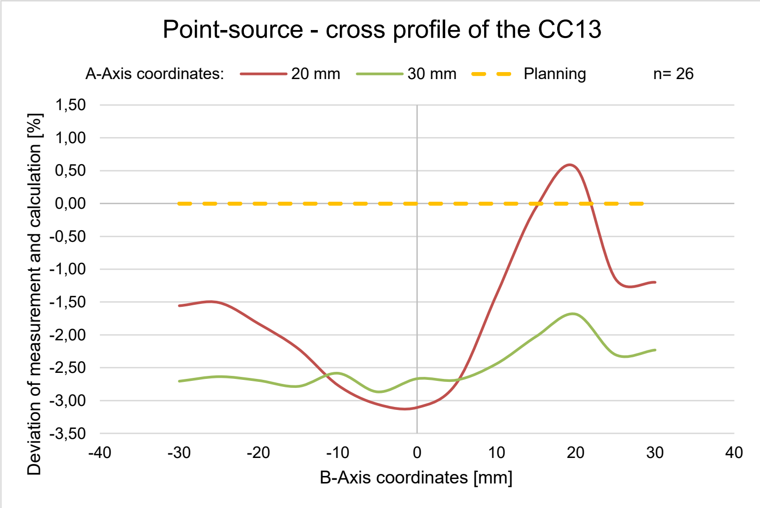

Figure 24: Diagram showing the deviation between the different Axis-coordinates A and B for the CC13. The different A-axis coordinates represent the depth dose. The B-axis represent the variation of the detector in the cross profile. The point dose was set at his max. Signal high.

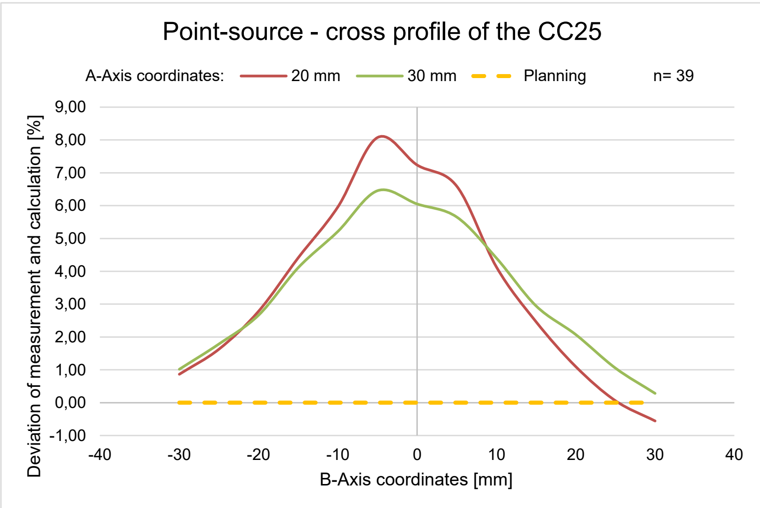

Figure 25: Diagram showing the deviation between the different Axis-coordinates A and B for the CC25. The different A-axis coordinates represent the depth dose. The B-axis represent the variation of the detector in the cross profile. The point dose was set at his max. Signal high.

3.3.4 "Active length" - depth dose irradiation

In these measurement tests, the CC04 and the CC13 showed the smallest deviation with 3 % variation around the design. With 6 %, the CC25 and RAZOR$^{\text{Nano Chamber}}$ were those with the highest deviation from the expected calculated measured value. Figures 26 and 27 did not show that the accuracy of the measurements would increase with an increase in the "active length".

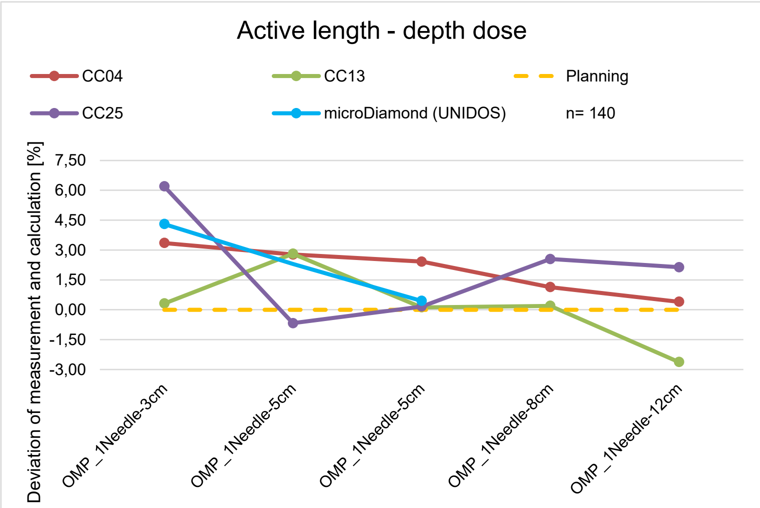

Figure 26: Diagram showing the deviations between calculated dose by the TPS (0,%) and measured doses. The active length was set for every detector individual and rise up form three to twelve mm.

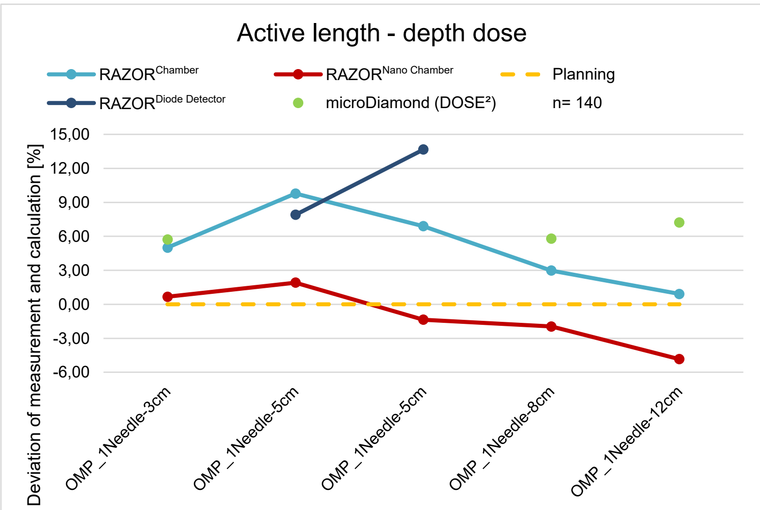

Figure 27: Diagram showing the deviations between calculated dose by the TPS (0,%) and measured doses. The "active length" was set for every detector individual and rise up form three to twelve mm.

3.3.5 "Active length" - cross profile irradiation

When evaluating the figure 28 it became obvious that with an "active length" of 3 cm the CC13 showed the smallest difference to the treatment planning. The microDiamond had its smallest deviation at an A-axis distance of 20 mm. At an irradiation length of 5 cm, see figures 29 and 30, the microDiamond the CC04 and CC25 showed the highest deviation at a B-axis of -10 to 10 mm. Increasing the A-axis again contributed to a convergence to treatment planning. The CC13 showed the best agreement with the calculated dose, whereby an increase in the distance in the A-axis no longer provided a large improvement. With an "active length" of 8 cm, CC13 was closest to the calculated dose, the microDiamond varied most in the B-axis range from -50 to 50 mm. Also again, see figure 31, that the higher distance to the needle (higher A-axis) provided an provided an improvement in the knife edge. Figure 32 showed a consistent deviation to the design for both detectors used.

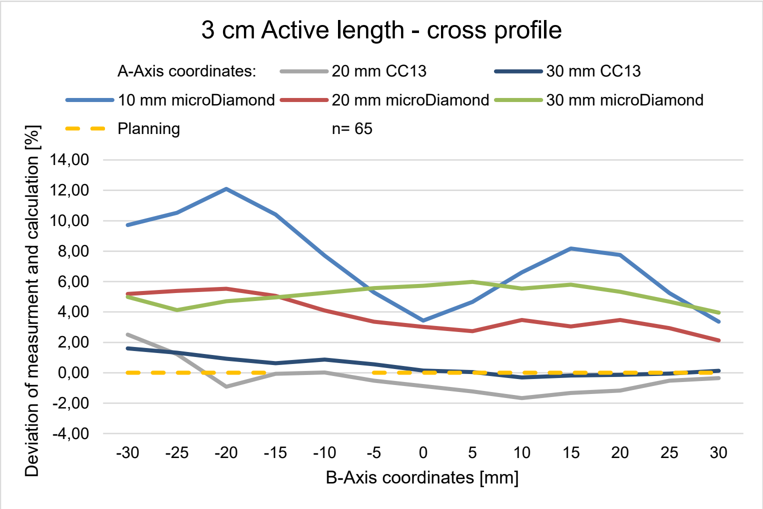

Figure 28: Diagram showing the deviations between calculated dose by the TPS (0,%) and measured doses when the A- and B-Axis coordinates rise up. The different A-axis coordinates represent the depth dose. The B-axis represent the variation of the detector in the cross profile.

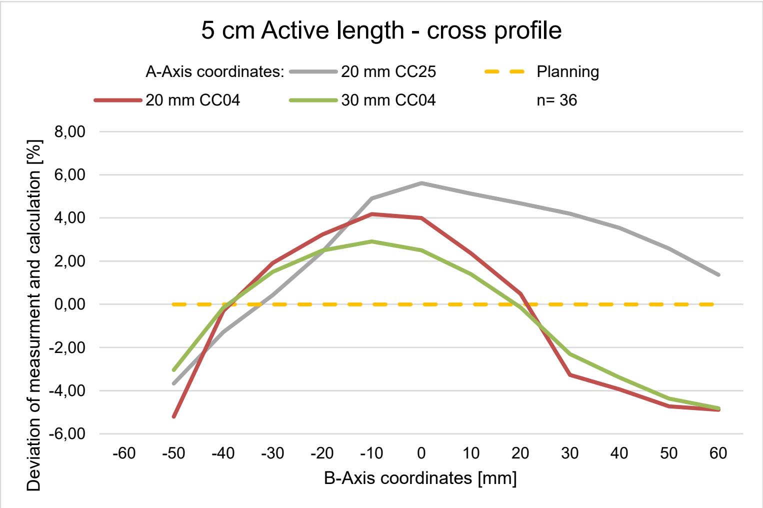

Figure 29: Diagram showing the deviations between calculated dose by the TPS (0,%) and measured doses when the A- and B-Axis coordinates rise up. The different A-axis coordinates represent the depth dose. The B-axis represent the variation of the detector in the cross profile.

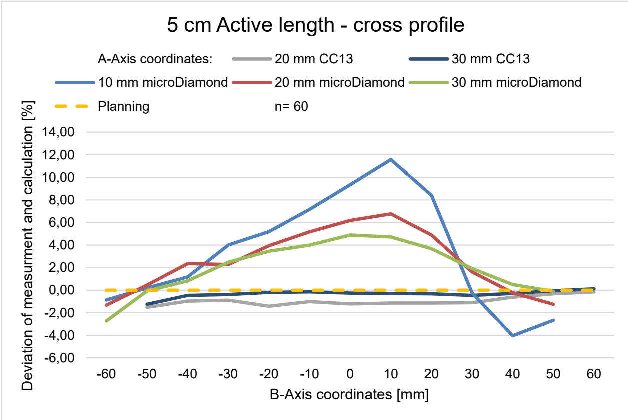

Figure 30: Diagram showing the deviations between calculated dose by the TPS (0,%) and measured doses when the A- and B-Axis coordinates rise up. The different A-axis coordinates represent the depth dose. The B-axis represent the variation of the detector in the cross profile.

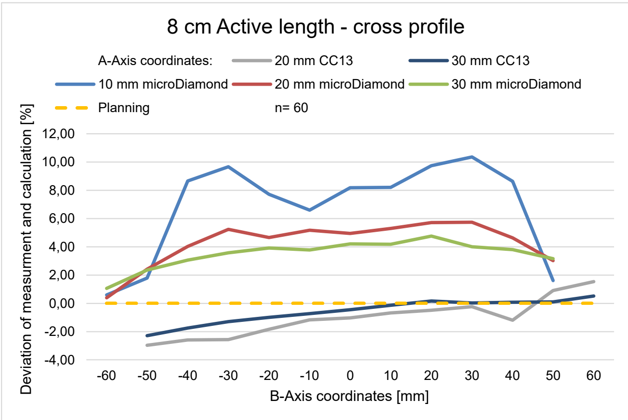

Figure 31: Diagram showing the deviations between calculated dose by the TPS (0,%) and measured doses when the A- and B-Axis coordinates rise up. The different A-axis coordinates represent the depth dose. The B-axis represent the variation of the detector in the cross profile.

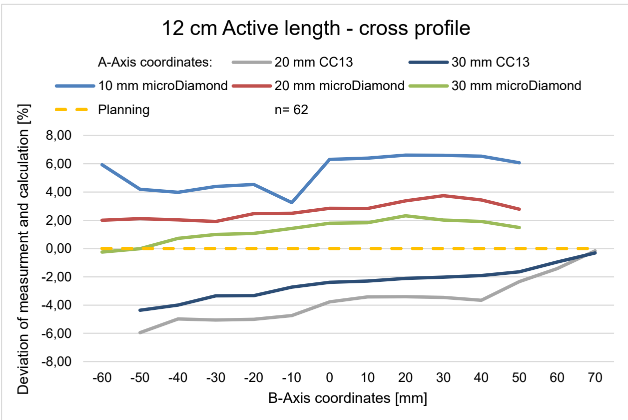

Figure 32: Diagram showing the deviations between calculated dose by the TPS (0,%) and measured doses when the A- and B-Axis coordinates rise up. The different A-axis coordinates represent the depth dose. The B-axis represent the variation of the detector in the cross profile.

3.3.6 5 needles in triangular configuration irradiation

For the 5 needles in triangular configuration (see figure 33), the best match to calculated dose was achieved with the CC25 at a C-axis spacing of 8 mm. The measurements showed that all the chambers used had the same measurement curve, and were only offset by a few percent. Furthermore, a higher C-axis distance did not lead to noticeably better measurement results.

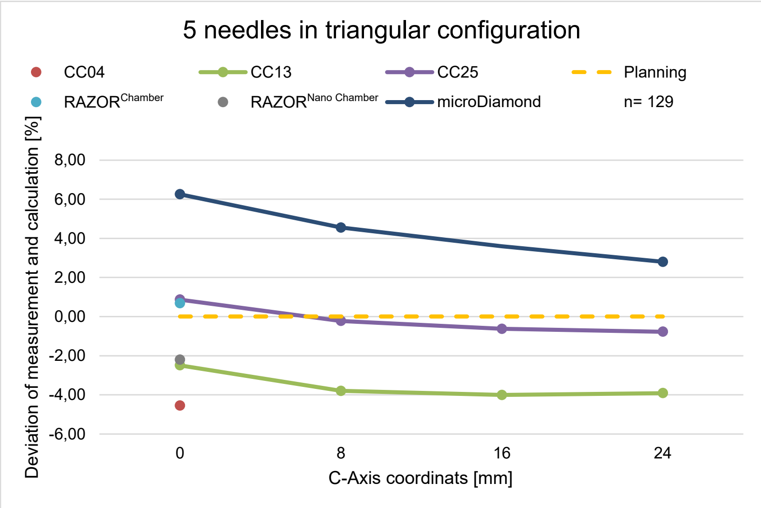

Figure 33: Diagram showing the deviations between calculated dose by the TPS (0,%) and measured doses when the C-Axis coordinate rise up from zero to twenty-four mm. The different C-axis coordinates represent the movement in horizontal direction.

3.3.7 Dependance on water heights irradiation

The CC13 showed a decrease in dose at a water height of 2.5 cm. The RAZOR Nano Chamber showed the decrease from 2.0 cm. Both chambers showed, as can be seen in figure 34, an increasing decrease of the dose with decreasing water height.

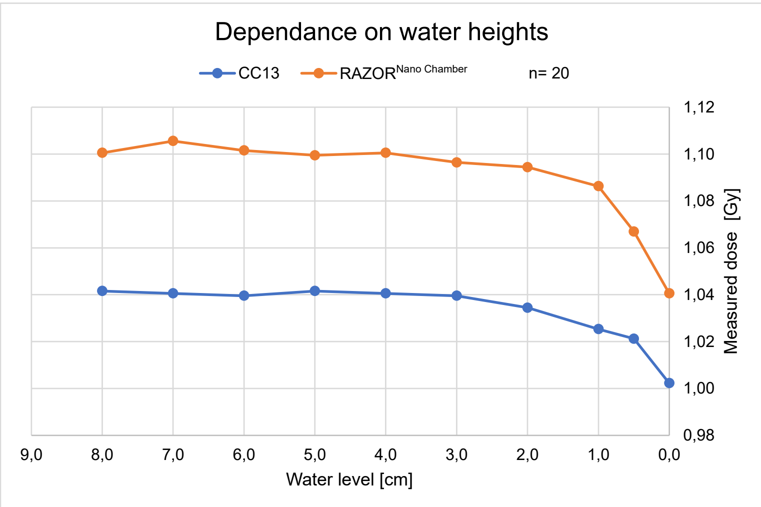

Figure 34: Diagram showing the measured dose by different water level.

3.3.8 Overview of all detectors

The CC04 (table 13) showed the lowest deviation from all measurements made with this chamber in the "active length" cross profile with mean 0.57 %. The 5 needles in triangular configuration had the highest deviation from treatment planning. When looking at the deviation of normalised data, it was noticeable that all measured values were below 1.5 % related to the mean values. The measurement with the lowest deviation was the dose linearity of point-source with mean 0.02 %. The highest value for the "active length" of cross profile was mean 1.22 %.

Table 13: Summary of all results for the measurements setups with the CC04 in the water phantom.

CC04			
Treatment	Parameter	Length measured $[mm]$	Length calculated (from figure) $[mm]$
Distance for the max. Signal		1132 $\pm$ 1	1130 $\pm$ 1
		Deviation $[\%]$	Deviation of normalised data $[\%]$
Dose linearity of point-source	Mean	2.29	**0.02**
	SD	0.06	0.05
	Min.	2.17	-0.03
	Max.	2.34	0.14
Point-source - depth dose	Mean	3.27	0.85
	SD	0.95	1.07
	Min.	1.95	0.00
	Max.	5.04	3.63
Active length - depth dose	Mean	2.12	0.65
	SD	1.36	0.87
	Min.	-0.53	-0.43
	Max.	4.93	3.31
Active length - cross profile	Mean	**-0.57**	**1.22**
	SD	3.15	1.68
	Min.	-5.21	-4.89
	Max.	4.18	3.88
5 needles in triangular configuration	Mean	**-4.55**	1.13
	SD	6.78	0.84
	Min.	-19.64	-0.05
	Max.	2.00	2.56

The CC13 (table 14) achieved its best result for the "active length" in the depth dose. The 5 needles in triangular configuration showed the largest difference to the calculated dose with mean -3.55 %. The deviation of normalised data of this chamber showed the lowest difference of mean -0.05 % for the "active length" by cross profile. With mean -0.85 %, the "point-source" depth dose was furthest away from the normalised values. Nevertheless, all deviations of normalised data were below 1 % related to the mean values. The measurement of max. signal showed a difference of 4 mm for the CC13 when comparing measurements and the drawing.

Table 14: Summary of all results for the measurements setups with the CC13 in the water phantom.

CC13			
Treatment	Parameter	Length measured $[mm]$	Length calculated (from figure) $[mm]$
Distance for the max. Signal		1132 ± 1	1128 ± 1
		Deviation $[\%]$	Deviation of normalised data $[\%]$
Dose linearity of point-source	Mean	-2.10	0.17
	SD	0.29	0.29
	Min.	-2.66	-0.03
	Max.	-1.91	0.74
Point-source - depth dose	Mean	0.57	**-0.85**
	SD	1.52	0.50
	Min.	-2.24	-1.54
	Max.	2.36	0.00
Point-source - cross profile	Mean	-2.09	-0.43
	SD	0.88	0.55
	Min.	-3.11	-1.97
	Max.	0.55	0.20
Active length - depth dose	Mean	**0.15**	0.10
	SD	2.15	1.25
	Min.	-6.36	-1.78
	Max.	3.42	4.51
Active length - cross profile	Mean	-1.13	**-0.05**
	SD	1.59	0.74
	Min.	-5.96	-3.89
	Max.	2.51	1.74
5 needles in triangular configuration	Mean	**-3.55**	-0.58
	SD	2.06	1.54
	Min.	-8.65	-2.06
	Max.	-0.78	4.07
		MS $[Gy]$	
Dependance on water heights	Mean	1.033	
	SD	0.012	
	Min.	1.002	
	Max.	1.042	

The CC25 (table 15) showed the most ideal match to the treatment planning with mean -0.05 % for the 5 needles in triangular configuration. For the dose linearity of "point-source" it was mean 6.68 % with an deviation of normalised data of mean -0.48 %. The "point-source" cross profile and 5 needles in triangular configuration with mean 0.33 % each were the measurements with the lowest deviations of normalised data. The "active length" cross profile measurement showed the highest deviation of normalised data with mean 0.89 %, whereby the chamber always showed an deviation of normalised data of < 1 % related to the mean values.

Table 15: Summary of all results for the measurements setups with the CC25 in the water phantom.

CC25			
Treatment	Parameter	Length measured $[mm]$	Length calculated (from figure) $[mm]$
Distance for the max. Signal		1129 $\pm$ 1	1127 $\pm$ 1
		Deviation $[\%]$	Deviation of normalised data $[\%]$
Dose linearity of point-source	Mean	**6.68**	-0.48
	SD	1.12	1.05
	Min.	6.11	-3.14
	Max.	9.51	0.06
Point-source - depth dose	Mean	5.40	-0.38
	SD	1.27	0.58
	Min.	3.15	-1.56
	Max.	6.75	0.55
Point-source - cross profile	Mean	5.21	**-0.33**
	SD	1.89	0.75
	Min.	2.72	-2.02
	Max.	8.90	0.74
Active length - depth dose	Mean	1.44	0.85
	SD	4.24	0.88
	Min.	-12.75	-0.83
	Max.	7.21	2.96
Active length - cross profile	Mean	2.49	**0.89**
	SD	2.73	1.45
	Min.	-3.67	-2.89
	Max.	5.62	2.83
5 needles in triangular configuration	Mean	**-0.05**	**0.33**
	SD	0.93	0.82
	Min.	-2.18	-0.23
	Max.	1.31	2.52

The RAZOR^{Chamber} (table 16) had its highest difference to the calculated dose for the "point-source" - depth dose, but the 5 needles in triangular configuration was at least mean 0.68 %. The deviations of normalised data were mean 0.04 % for the dose linearity of point-source measurement and mean 1.42 % for "active length" depth dose. It was found that the deviations of normalised data were always below 1.5 % related to the mean values for this chamber.

Table 16: Summary of all results for the measurements setups with the RAZOR^{Chamber} in the water phantom.

RAZOR^{Chamber}			
Treatment	Parameter	Length measured $[mm]$	Length calculated (from figure) $[mm]$
Distance for the max. Signal		1129 $\pm$ 1	1128 $\pm$ 1
		Deviation $[\%]$	Deviation of normalised data $[\%]$
Dose linearity of point-source	Mean	6.54	**0.04**
	SD	0.02	0.02
	Min.	6.51	0.00
	Max.	6.58	0.06
Point-source - depth dose	Mean	**6.68**	0.60
	SD	1.47	0.28
	Min.	4.11	0.00
	Max.	9.00	1.06
Active length - depth dose	Mean	5.72	**1.42**
	SD	3.92	2.25
	Min.	-2.13	0.00
	Max.	11.02	15.99
5 needles in triangular configuration	Mean	**0.68**	0.65
	SD	1.72	0.52
	Min.	-2.35	-0.37
	Max.	2.89	1.21

For the RAZOR$^{\text{Nano Chamber}}$ (table 17), the measurements of the dose linearity of "point-source", showed the highest deviation to the treatment planning with mean 5.25 %. The "active length" by depth dose measurements showed the smallest difference for this chamber with mean -0.72 %. The comparison of the deviation of normalised data showed that the dose linearity of "point-source" had the lowest value with mean 0.04 %. With mean 1.57 %, the measurements of the "point-source" depth dose was the highest in summary. This chamber achieved deviations of normalised data of less than 2 % related to the mean values.

Table 17: Summary of all results for the measurements setups with the RAZOR$^{\text{Nano Chamber}}$ in the water phantom.

RAZOR$^{\text{Nano Chamber}}$			
Treatment	Parameter	Length measured $[mm]$	Length calculated (from figure) $[mm]$
Distance for the max. Signal		1129 ± 1	1127 ± 1
		Deviation $[\%]$	Deviation of normalised data $[\%]$
Dose linearity of point-source	Mean	**5.25**	**0.04**
	SD	0.10	0.10
	Min.	5.00	-0.09
	Max.	5.39	0.28
Point-source - depth dose	Mean	1.91	**1.57**
	SD	4.15	0.87
	Min.	-4.23	0.00
	Max.	7.73	3.12
Active length - depth dose	Mean	**-0.72**	1.28
	SD	3.89	1.01
	Min.	-10.57	-0.66
	Max.	4.97	2.98
5 needles in triangular configuration	Mean	-2.20	1.50
	SD	3.37	0.86
	Min.	-7.85	0.00
	Max.	1.92	2.39
		MS $[Gy]$	
Dependance on water heights	Mean	1.089	
	SD	0.019	
	Min.	1.041	
	Max.	1.106	

For the RAZOR$^{\text{Diode Detector}}$ (table 18) one measurement setup was looked at. It is visible that the deviation for the "active length" at depth-dose was mean 10.3 % with an deviation of normalised data of mean -0.22 %.

Table 18: Summary of all results for the measurements setups with the RAZOR$^{\text{Diode Detector}}$ in the water phantom.

RAZOR$^{\text{Diode Detector}}$			
Treatment	Parameter	Length measured $[mm]$	Length calculated (from figure) $[mm]$
Distance for the max. Signal		1119 ± 1	1118 ± 1
		Deviation $[\%]$	Deviation of normalised data $[\%]$
Active length - depth dose	Mean	**10.30**	**-0.22**
	SD	4.78	4.88
	Min.	4.13	-7.63
	Max.	23.59	16.24

In the case of the microDiamond (table 19), the measurements were carried out with different electrometers. The comparison of the measurements showed that for both the Unidos and the Dose^2 the highest deviation was found in the "point-source" depth dose measurements. No systematic difference for the Unidos and Dose^2 electrometer could be found.

The microDiamond in combination with the Unidos showed the best agreement to the calculated dose for the "active length" depth dose. For the Dose^2, the measurements of the "active length" at cross profile with mean 3.70 % was the measurement that showed the smallest difference to the calculated dose.

When comparing the deviations of normalised data, for the microDiamond with both electrometers, the lowest measured values were mean -1.25 % (Unidos) and mean 0.62 % (Dose^2). For the "active length" depht dose, the detector for the measurements with the Unidos achieved the highest deviation of normalised data of mean 1.86 %.

The combination of microDiamond and Dose^2 achieved the most striking difference of mean -32.90 % for the "point-source" depth dose. This high deviation resulted from the fact that the microDiamond was at a distance of 5 mm from the source. As a result, the detector received more dose than was actually planned.

The measured deviations of normalised data were in a value range of less than 5 % related to the mean values.

Table 19: Summary of all results for the measurements setups with the microDiamond in the water phantom.

microDiamond			
Treatment	Parameter	Length measured $[mm]$	Length calculated (from figure) $[mm]$
Distance for the max. Signal		1119 $\pm$ 1	1118 $\pm$ 1
		Deviation $[\%]$	Deviation of normalised data $[\%]$
Point-source - depth dose	Mean (Unidos)	**8.55**	
	SD (Unidos)	4.66	
	Min. (Unidos)	3.95	
	Max. (Unidos)	17.63	
	Mean (Dose^2)	**8.89**	**-32.90**
	SD (Dose^2)	7.41	90.59
	Min. (Dose^2)	3.71	-303.66
	Max. (Dose^2)	28.87	0.99
Point-source - cross profile	Mean	3.54	1.41
	SD	3.40	0.93
	Min.	-1.60	-0.70
	Max.	13.38	4.02
Active length - depth dose	Mean (Unidos)	**2.37**	**-1.86**
	SD (Unidos)	2.25	4.98
	Min. (Unidos)	-0.40	-18.25
	Max. (Unidos)	6.80	0.46
	Mean (Dose^2)	6.25	-4.82
	SD (Dose^2)	3.29	13.09
	Min. (Dose^2)	3.41	-51.88
	Max. (Dose^2)	18.55	0.71
Active length - cross profile	Mean (Unidos)	5.55	**-1.25**
	SD (Unidos)	2.71	1.33
	Min. (Unidos)	2.12	-4.59
	Max. (Unidos)	12.09	0.34
	Mean (Dose^2)	**3.70**	**0.62**
	SD (Dose^2)	2.81	0.95
	Min. (Dose^2)	-4.04	-1.96
	Max. (Dose^2)	11.58	3.70
5 needles in triangular configuration	Mean	4.46	-0.96
	SD	1.81	4.35
	Min.	1.83	-23.24
	Max.	12.37	5.42

4 Discussion

Furthermore, the subdivision enables a better comparison of the detectors with regard to their accuracies and advantages. To highlight all these features, the detectors are subdivided into:

- Semiconductor detectors
  - Semiconductor detector T9112 (Rectum)
  - Semiconductor detector T9113 (Bladder)
  - $\text{RAZOR}^{\text{Diode Detector}}$
- Ionisation chambers
  - CC04
  - CC13
  - CC25
  - $\text{RAZOR}^{\text{Chamber}}$
  - $\text{RAZOR}^{\text{Nano Chamber}}$
  - 0.3 cm^3 Semiflex Chamber
- Diamond detector
  - microDiamond

4.1 Analysis of the semiconductor detectors results

The semiconductor detectors T9112 and T9113 show higher deviation to the values of the treatment planning. Whereas in the measurement results of the table 4 the Measurement Series (MS) 4 of the rectum probe shows significantly lower deviations. In the case of MS 4, the cables of the rectum and bladder probe were deliberately twisted in the course of the measurement in order to check whether the position of the diode cables had an influence on the sensitivity of the diodes. The positioning of the diode cables does not play a role as can be seen from the data of the measurement, which can be found in the appendix under "A; In-vivo phantom Data". A comparison of the results of an earlier study with the same semiconductor detectors by Waldhäusl et al. confirms this assumption. Here, deviations between the measured dose of the detectors and the calculated dose of the treatment planning were achieved with an average of $4.9 \pm 3\,\%$ [33].

The linearity of the semiconductor detector's shows a drop at 0.5 Gy as can be seen in figure 13. A close examination of the measured values for exactly that range revealed a variation between the previous (0.25) and subsequent measurement (1) of 0.002 to 0.008 Gy. This deviation is so small that it can be declared as normal measurement fluctuations. Thus, the semiconductor detectors T9112 and T9113 show a linear behaviour.

In the measurements with the RAZOR$^{\text{Diode Detector}}$ in particular the direct comparison between the results of the needle phantom (table 10) and the water phantom (table 18) shows, that the detector in the needle phantom achieves the smaller deviations to the calculated dose. For the needle phantom, a value of less than 1 % was measured related to the mean values. This value refers to both the deviation between measured and calculated doses and the deviation of the normalised data. However, for the comparative measurements with "active length", the deviation is about 3.03 % (see table 10).

No reason can be given for the higher deviation of the comparative measurements with "active length". However, it can be assumed that this measurement result is an outlier because the comparative measurements with "point-source" always delivered good results with all two MS. Furthermore, the RAZOR$^{\text{Diode Detector}}$ always showed very small deviations from the treatment planning when measuring different "active lengths". To check whether this was an outlier, further measurements should be carried out.

4.2 Analysis of the ionisation chambers results

For measurements in the water phantom, the CC chambers achieved better measurement results than the RAZOR chambers. Depending on the treatment, the deviation for the CC's was about 0.05-6.68 % (see table 15) and for the RAZOR's about 0.68-6.68 % (see table 16). This slightly higher deviation of the RAZOR's corresponds well to a comparable study by Ballester et al. where the existing measured values of a pinpoint chamber (volume 0.015 cm^2) using the Monte Carlo method were compared. Maximum deviation of 10 % was calculated there [34].

In terms of deviation of normalised data, all ion chambers show measured values of less than 2 % (see table 13-17). This is in contrast to the results of the needle phantom measurements where all CC's and RAZOR chambers show the lowest deviation from treatment planning, by comparison needle and water phantom.

When comparing the CC's, it is noticeable that the CC04 has performed the worst of all CC's, despite its low volume of 0.04 cm^2. Moura et al. carried out an investigation with an A1SL (volume 0.053 cm^2) that is similar to the dose linearity of "point-source". In the experiment of Moura et al. a mean deviation from treatment planning of 4.81 % was calculated [35].

The CC04 show a deviation of 5.93 % (see table 5) for the linearity of "point-source" measurement. The RAZOR's also show a higher deviation from the calculated dose for the chambers with lower volumes, this can seen in the graphs 18 and 19. However, this does not affect the deviation of normalised data, which achieves good measurement results for all ion chambers.

The comparison of the linearity of the water phantom (figure 21) and needle phantom (figure 16 and 17) shows that all detectors have a linear behaviour above from a certain irradiation level. Except the microDiamond and the RAZOR$^{\text{Diode Detector}}$ these always showed a linear behaviour from the beginning of the measurements. Due to its design and the resulting physical behaviour, the RAZOR$^{\text{Diode Detector}}$ does not require any pre-irradiation for the detection of radiation. For the microDiamond and the ionisation chambers, a basic irradiation is recommended/required by the manufacturer (microDiamond). In the case of the diamond, this can be explained by the fact that the traps have to be filled with electrons [27], [20, pp. 89–91], [5, pp. 173–175, 167]. For ionisation chambers it has been observed for a long time that pre-irradiation provides better measurement results. This observation was investigated in detail by McCaffray et al. in a study that identified radiation-induced conductivity as the physical cause necessary pre-irradiation [36]. The deviations at the beginning of the linearity study can be explained by the fact that the CC's basic irradiation was not taken into account, although even some manufacturers refer to it in their operating instructions[22], [23], [21], [24], [25]. This was improved during the study.

In the experiments where "active length" were irradiate, it can be seen that the chambers whit small active volume show better agreement to the treatment planning when the "active length" increases. This can be seen in the figures 26 and 27. There is definitely a correlation between "active length" and active volume of the different chambers. This could be due to the higher sensitivity of the small-volume chambers.

In the course of the investigation, it was further noticed that with increasing distance to the source, the agreement with the treatment planning coincided. At a distance of more than 90 mm the deviations began to increase again until 6.04 % at 140 mm (measured with CC25 see appendix C; "Summary depth-dose - Length (3, 5, 8, 12 cm) in the water phantom"). This tendency was also already observed by Vensella et al. and Gromoll et al. [37], [38]. Whereas Vensella applied its distance in the clinically relevant range of 0 to 60 mm and Gromoll measured further up to 180 mm. In the close range of 5 to 15 mm, the microDiamond and the RAZOR$^{\text{Diode Detector}}$ achieved deviations of 0.16-18.55 % (see also the appendix C; "Summary depth-dose - Length (3, 5, 8, 12 cm) in the water phantom"), respectively, and were thus significantly worse than the measurements with a distance of more than 15 mm. This is also in line with the investigations of Vensella and Gromoll.

4.3 Analysis of the diamond detector results

When comparing the results of the needle and water phantom for the microDiamond the deviation between measured and calculated dose as well the normalised data in the needle phantom is again less than 1 %, relate to the mean values. For the comparative measurement with "active length" the deviation is mean 1.19 % (see table 12). This value may be an outlier, as both the previous measurements of the comparative Measurement with "point-source" and the treatment different "active length" show a much better agreement with the treatment planning. Further measurements with the treatment comparative measurement with "active length" would have been necessary to prove this.

In the measurements with the water phantom, the conformity between measured and calculated dose was not as good as with the needle phantom. This is expressed by the larger difference between both deviations with a value of approximately 10 %, related to the mean values (see table 19). This can be explained by the smaller distances between the source and the microDiamond detector.

Laub et al. found that the microDiamond provides very good measurement results for measurements in teletherapy [39]. Based on the measurement results from the study by Laub et al., the microDiamond delivers very good results for the Brachytherapy too. This shows that the microDiamond is also suitable for brachytherapy.

4.4 Conclusion of the investigations

In conclusion, the following essential findings can be summarised from the observed behaviour of the detectors:

- All detectors, with the exception of the semiconductor detectors, require a basic irradiation due to the physical properties of the detectors. Only when this is given, the detectors deliver solid results.
- The type of irradiation "point-source" and "active length" plays an important role for the measurement results. Depending on the chamber used, this fact contributes to the correlation between measured and calculated dose.
- The measurements show a very good agreement with the treatment planning. This applies especially to the clinically relevant dose range of 15 to 50 mm.
- Chambers with a larger active volume achieve for some experimental setups better results on average. This does not mean, however, that chambers with small active volume are

unsuitable. Because of the steep dose gradient this could not been foreseen when starting the measurements. The study shows, that all chambers can be used.

- The measurements with the needle phantom show very good agreement to the results of the TPS. The water phantom shows sometimes higher deviations. The advantage of the needle phantom is the easy and reproducible usage in fixed geometry. The advantage of the much more complex water phantom is, that if offers more possibilities of measuring the dose in each distance.

In summary, it can be said that (1) all detectors used in this study can be used for further dose measurements in brachytherapy. Both, the deviations (mean 0.05 to 10 %) and the deviations of normalised data (mean < 2 %) demonstrate very good measurement results. Special care has to be given to the RAZOR chambers, they should rather be used for deviations measurements and not for deviations of normalised data measurements.
The study shows (2) that the use of the needle phantom enables precise measurements with simultaneous easy handling of the phantom. Since the measurement effort is very manageable with a significant improvement of routinely performed Quality Assurance (QA). Therefore it is also recommended for brachytherapy to be include for regular comparative measurement between calculated dose and measured dose in the standard S 5296 [4].
The study also showed, that (3) the verification of TPS measurements with the water phantom provides an additional control that would help to increase safety for the patient and is recommend for commissioning of TPS.

Bibliography

References

[1] S. Biani et al., *IAEA Human health series Nr. 30 - Implementation of High Dose Rate Brachytherapy in Limited Resource Settings*, E. Fidarova and E. Rosenblatt, Eds. Wien, Austria: International Atomic Energy Agency, 2015. [Online]. Available: https://www-pub.iaea.org/MTCD/Publications/PDF/Pub1670web-5444797.pdf (visited on 02/16/2021).

[2] *Klinische Dosimetrie Teil 1: Allgemeines zur Dosimetrie in der Tele- und Brachytherapie*, ÖNORM S 5234-1, Österreichisches Normungsinstitut, Wien, Austria, Dec. 1, 2002.

[3] *Bestrahlungsplanungssysteme: Konstanzprüfung von Qualitätsmerkmalen*, ÖNORM S 5295, Österreichisches Normungsinstitut, Wien, Austria, Jun. 1, 2015.

[4] *Bestrahlungsplanungssysteme: Abnahmeprüfung von Qualitätsmerkmalen*, ÖNORM S 5296, Österreichisches Normungsinstitut, Wien, Austria, Nov. 1, 2008.

[5] H. Krieger and W. Petzold, *Strahlenphysik, Dosimetrie und Strahlenschutz: Band 2 Strahlungsquellen, Detektoren und klinische Dosimetrie*, 2nd ed. Stuttgart, Germany: B. G. Teubner, 1997, vol. 2.

[6] P. Bachert et al., *Medizinische Physik: Grundlagen - Bildgebung - Therapie - Technik*, W. Schlegel, C. P. Karger, and O. Jäkel, Eds. Berlin, Germany: Springer-Verlag GmbH, 2018.

[7] M. Behe et al., *Radiologie: Bildgebende Verfahren, Strahlentherapie, Nuklearmedizin und Strahlenschutz*, 4th ed., G. Kauffmann, R. Sauer, and W. Weber, Eds. München, Germany: Elsevier GmbH, 2011.

[8] T. Block et al., *Praktisches Handbuch der Brachytherapie*, 2nd ed., V. Strnad, R. Pötter, and G. Kovács, Eds. Bremen, Germany: UNI-MED Verlag AG, 2010.

[9] J. Perez-Calatayud et al., *Dose Calculation for Photon-Emitting Brachytherapy Sources with Average Energy Higher than 50 keV: Full Report of the AAPM and ESTRO*. Maryland, United States of America: American Association of Physicists in Medicine, 2012.

[11] R. Nath, L. L. Anderson, G. Luxton, K. A. Weaver, J. F. Williamson, and A. S. Meigooni, "Medical Physics," *Dosimetry of interstitial brachytherapy sources: Recommendations of the AAPM Radiation Therapy Committee Task Group No. 43*, vol. 22, no. 2, pp. 209–234, Feb. 1995. DOI: https://doi.org/10.1118/1.597458.

[12] D. Baltas and J. Vensellar, *The GEC ESTRO Handbook of Brachytherapy PART I: THE BASICS OF BRACHYTHERAPY*, 2nd ed. Brussels, Belgium: European Society of Therapeutic Radiology and Oncology (ESTRO), 2014.

[13] J. Perez-Calatayud, F. Ballester, R. K. Das, L. A. DeWerd, G. S. Ibbott, A. S. Meigooni, Z. Ouhib, M. J. Rivard, R. S. Sloboda, and J. F. Williamson, "Medical Physics," *Dose calculation for photon-emitting brachytherapy sources with average energy higher than 50 keV: Report of the AAPM and ESTRO*, vol. 39, no. 5, pp. 2904–2929, May 2012. DOI: https://doi.org/10.1118/1.3703892.

[14] R. Al-Mazrou et al., *Nuclear medicine physics: A handbook for teachers and students*, D. L. Bailey, J. L. Humm, A. Todd-Pokropek, and A. van Aswegen, Eds. Wien, Austria: International Atomic Energy Agency, 2014.

[15] H. Krieger and W. Petzold, *Strahlenphysik, Dosimetrie und Strahlenschutz: Band 1 Grundlagen*, 4th ed. Wiesbaden, Germany: Springer Fachmedien, 1998, vol. 1.

[16] K. A. Fonseca, M. F. Koskinas, and M. S. Dias, "Applied radiation and isotopes," *Disintegration rate measurement of a 192Ir solution*, vol. 54, no. 1, pp. 141–145, Jan. 2001. DOI: https://doi.org/10.1016/S0969-8043(00)00158-5.

[17] "Iridium-192," OncologyMedicalPhysics.com. (), [Online]. Available: https://oncologymedicalphysics.com/iridium-192/ (visited on 03/14/2021).

[18] J. Yang, "Medical dosimetry," *Oncentra brachytherapy planning system*, vol. 43, no. 2, pp. 141–149, Jun. 2018. DOI: https://doi.org/10.1016/j.meddos.2018.02.011.

[19] D. Granero, J. Pérez-Calatayud, E. Casal, F. Ballester, and J. Venselaar, "Medical physics," *A dosimetric study on the Ir-192 high dose rate flexisource*, vol. 33, no. 12, pp. 4578–4582, Dec. 2006. DOI: https://doi.org/10.1118/1.2388154.

[20] H. Krieger, *Strahlungsmessung und Dosimetrie*, 2nd ed. Wiesbaden, Germany: Springer Fachmedien, 2013.

[31] *Klinische Dosimetrie: Bestimmung der Kenndosisleistung in der Brachytherapie mit umschlossenen gammastrahlenden radioaktiven Stoffen*, ÖNORM S 5234-2, Österreichisches Normungsinstitut, Wien, Austria, May 1, 2001.

[32] H. Krieger and D. Baltas, "Praktische dosimetrie in der HDR-brachytherapie," Deutsche Gesellschaft für Medizinische Physik e.V. (DGMP), Ingolstadt and Offenbach, Germany, 2006. [Online]. Available: https://www.dgmp.de/media/document/199/Bericht13-Korr-Auflage-2006-2-.pdf (visited on 02/01/2021).

[33] C. Waldhäusl, A. Wambersie, R. Pötter, and D. Georg, "Radiotherapy and Oncology: Journal of the European Society for Therapeutic Radiology and Oncology," *In-vivo dosimetry for gynaecological brachytherapy: Physical and clinical considerations*, vol. 77, no. 3, pp. 310–317, Dec. 2005. DOI: https://doi.org/10.1016/j.radonc.2005.09.004.

[34] F. Ballester, J. Perez-Calatayud, and V. Puchades, "Physics in medicine and biology," *Comments on 'determination of the dose characteristics in the near area of a new type of 192Ir-HDR afterloading source with a pinpoint ionization chamber'*, vol. 48, no. 5, L23–25, author reply L25–26, Mar. 2003. DOI: 10.1088/0031-9155/48/5/101.

[35] E. S. Moura, J. A. Micka, C. G. Hammer, W. S. Culberson, L. A. DeWerd, M. E. C. M. Rostelato, and C. A. Zeituni, "Medical Physics," *Development of a phantom to validate high-dose-rate brachytherapy treatment planning systems with heterogeneous algorithms*, vol. 42, no. 4, pp. 1566–1574, Apr. 2015. DOI: https://doi.org/10.1118/1.4914390.

[36] J. P. McCaffrey, B. Downton, H. Shen, D. Niven, and M. McEwen, "Physics in medicine and biology," *Pre-irradiation effects on ionization chambers used in radiation therapy*, vol. 50, no. 13, N121–N133, Jun. 2005. DOI: https://doi.org/10.1088/0031-9155/50/13/N01.

[37] J. L. Venselaar, P. H. van der Giessen, and W. J. Dries, "Medical Physics," *Measurement and calculation of the dose at large distances from brachytherapy sources: Cs137, Ir192, and Co60*, vol. 23, no. 4, pp. 537–543, Apr. 1996. DOI: https://doi.org/10.1118/1.597811.

[38] C. Gromoll and A. Karg, "Physics in medicine and biology," *Determination of the dose characteristics in the near area of a new type of 192Ir-HDR afterloading source with a PinPoint ionization chamber*, vol. 47, no. 6, p. 875, Mar. 2002. DOI: 10.1088/0031-9155/47/6/302.

[39] W. U. Laub and R. Crilly, "Journal of Applied Clinical Medical Physics," *Clinical radiation therapy measurements with a new commercial synthetic single crystal diamond detector*, vol. 15, no. 6, pp. 92–102, Jun. 2014. DOI: https://doi.org/10.1120/jacmp.v15i6.4890.

User Manuals

[10] *Flexitron® HDR Benutzerhandbuch*, Nucletron B.V. daughter company from Elekta AB, TH Veenendaal, Netherlands, 2016.

[21] *CC25 Ionization Chamber User's Guide*, IBA Dosimetry GmbH, Schwarzenbruck, Germany, 2014.

[22] *CC04 Ionization Chamber User's Guide*, IBA Dosimetry GmbH, Schwarzenbruck, Germany, 2018.

[23] *CC13 Ionization Chamber User's Guide*, IBA Dosimetry GmbH, Schwarzenbruck, Germany, 2013.

[24] *RAZOR Chamber User's Guide*, 3rd ed., IBA Dosimetry GmbH, Schwarzenbruck, Germany, 2020.

[25] *RAZOR Nano Chamber User's Guide*, 4th ed., IBA Dosimetry GmbH, Schwarzenbruck, Germany, 2020.

[26] *RAZOR Detector User's Guide*, 4th ed., IBA Dosimetry GmbH, Schwarzenbruck, Germany, 2020.

[27] *Gebrauchsanweisung microDiamond Typ 60019*, PTW-FREIBURG Physikalisch-Technische Werkstätten Dr. Pychlau GmbH, Freiburg, Germany, 2019.

[28] *DETECTORS Including Codes of Practice*, PTW-FREIBURG Physikalisch-Technische Werkstätten Dr. Pychlau GmbH, Freiburg, Germany, 2016.

[29] *DOSE² Benutzerhandbuch*, IBA Dosimetry GmbH, Schwarzenbruck, Germany, 2018.

[30] *User Manual UNIDOS PTW-Universal Dosemeter*, PTW-FREIBURG Physikalisch-Technische Werkstätten Dr. Pychlau GmbH, Freiburg, Germany, 2009.

List of Figures

List of Tables

List of Abbreviations

AAPM American Association of Physicists in Medicine

B Bladder probe

CT Computed Tomography

CV Coefficient of Variation

DNA Deoxyribonucleic acid

EC Electron Capture

HDR High Dose Rate

MS Measurement Series

N Needle number

ND,W Calibration factor from "Eichstelle" (Dosiemtrielabor Seibersdorf) $N_{D,W}$

OMP Oncentra Masterplan

PDF Portable Document Format

PMMA Polymethylmethycrylat

pTP Air density correction factor p_{TP} = k_P

QA Quality Assurance

R Rectum probe

SD Standard Derivation

TCC Treatment Communication Console

TCP Treatment Control Panel

TDU Treatment Delivery Unit

TPS Treatment Planning System

Appendices

A In-vivo phantom Data

Table 20: Overview about the different project procedure for the in-vivo phantom. The values in the table stand for the measurement days, the year was omitted.

Treatment	Semiconductor detector T9112 (Rectum)	Semiconductor detector T9113 (Bladder)
Measurements	14.01. 15.01.	14.01. 15.01.
Dose linearity	15.01.	15.01.
Number of measurements(n)	20	20

Summary of the results measurments in the in-vivo phantom

Treatment plan		Ion chamber		Electrometer	
OMP Plan	OMP_Daniela_14.01.2021	Manufacturer	PTW	Manufacturer	PTW
TCC Plan	Daniela HDR	Model	Semiconductor detectors bladder	Model	VIVODOS
Phantom	in-vivo	SN	001291	SN	000327
Source calibration data		Manufacturer	PTW		
Date	28.10.2020	Model	Semiconductor detectors rectum		
Aktivity [Ci]	12.89	SN	002360		
SN	NLF01D85E5606				

PTW-fn = PTW-File name
R = Rectum probe
B = Bladder probe
SD = Standard deviation

Measurement Series 1							
PTW-fn	Probe set	R1 [Gy]	R2 [Gy]	R3 [Gy]	R4 [Gy]	R5 [Gy]	B [Gy]
Daniela-B_1	B	0.557	0.830	1.174	1.343	1.231	1.143
Daniela-B_2	B	0.556	0.829	1.171	1.340	1.229	1.145
Daniela-B_3	B	0.556	0.829	1.171	1.337	1.224	1.144
Mean		0.556	0.829	1.172	1.340	1.228	1.144
SD		0.0005	0.0005	0.0014	0.0024	0.0029	0.0008

	Date	[]	14.01.2021
Plan	Source aktivity	[Ci]	6.19
Plan	Total traeatment time	[s]	256
	Method	[]	Timed continuous
	Range	[]	-
	Length	[mm]	1270 - 1300

Measurement Series 4								
PTW-fn	Probe set	R1 [Gy]	R2 [Gy]	R3 [Gy]	R4 [Gy]	R5 [Gy]	B [Gy]	
Daniela-B_10	B	0.586	0.837	1.105	1.319	1.247	1.104	
Daniela-B_11	B	0.557	0.808	1.080	1.243	1.204	1.085	Cables of the probes change*
Daniela-B_12	B	0.542	0.783	1.067	1.214	1.129	1.089	
Daniela-B_13	B	0.532	0.775	1.095	1.274	1.232	1.076	
Daniela-B_14	B	0.541	0.783	1.064	1.221	1.124	1.142	
Mean		0.552	0.797	1.082	1.254	1.187	1.099	
SD		0.0190	0.0228	0.0158	0.0386	0.0515	0.0232	

	Date	[]	15.01.2021
Plan	Source aktivity	[Ci]	6.14
Plan	Total traeatment time	[s]	256
	Method	[]	Timed continuous
	Range	[]	-
	Length	[mm]	1270 - 1300

*Twist the cables of the probes to check whether the signal cables of the probes have an influence on the measurement results.

Difference between calculation and measurements						
Setup	R1 [%]	R2 [%]	R3 [%]	R4 [%]	R5 [%]	B [%]
Planning [Gy]	0.533	0.766	1.084	1.239	1.081	1.158
MS 1	4.4	8.2	8.1	8.2	13.6	-1.2
MS 2	6.0	10.2	7.6	8.7	15.6	-2.9
MS 3	10.1	9.4	2.1	6.6	15.4	-4.6
MS 4	3.5	4.0	-0.2	1.2	9.9	-5.1
Mean	6.0	8.0	4.4	6.2	13.6	-3.5
SD	2.5	2.4	3.5	3.0	2.3	1.5

B Needle phantom Data

Table 21: Overview about the different project procedure for the needle phantom. The values in the table stand for the measurement days, the year was omitted.

Treatment	CC04	CC13	CC25	RAZOR Chamber	RAZOR Nano	RAZOR Diode	micro-Diamond	0.3 cm^3 Semiflex
max. Signal	20.01.	21.01.	29.01.	17.02.	11.02.	19.02.	24.02.	23.02. 24.02
Dose linearity of point-source	10.02.	29.01.	29.01.	17.02.	11.02.	19.02.	24.02.	23.02.
Different active lengths	12.02.	17.02.	12.02.	19.02.	12.02.	19.02.	24.02.	23.02.
Comparative measurements	10.03. 09.04.	10.03. 09.04.	10.03. 09.04.	09.04.	10.03. 09.04.	09.04.	10.03. 09.04.	10.03. 09.04.
Comparative of 2 and 4 needle	29.04.	30.04.	30.04.					
Number of measurements(n)	295	218	252	117	114	72	158	141

Results of the comparative measurements in the needle phantom

Treatment plan		Ion chamber		
OMP Plan	see Table	Manufacturer	-	
TCC Plan	NORM_4Nadeln HDR	Model	see Table	
Phantom	Needle	SN	-	
Source calibration data		Electrometer		
Date	07.01.2021	Manufacturer	iba	PTW
Aktivity [Ci]	11.10	Model	Dose²	UNIDOS (A)
SN	NLF01D85E5930	SN	00298	10273

OMP = Oncentra Masterplan
N = Needle number

Chamber	Length [mm]	Time per position [s]	N1 [Gy]	N2 [Gy]	N3 [Gy]	N4 [Gy]	N4 correction with p_{TP} [Gy]	Mean [Gy]	Planning [Gy]	Deviation [%]	
iba CC04 SN 16286 (andere Kammer)	1110	130	0.636	1.224	1.831	2.422	2.460	2.459	2.456	0.11	
			0.636	1.224	1.829	2.419	2.457				
iba CC13 SN 16296	1111	130	0.573	1.147	1.782	2.456	2.495	2.496	2.456	1.62	
			0.573	1.147	1.783	2.458	2.497				
iba CC25 SN 16125	1113	130	0.563	1.128	1.757	2.427	2.466	2.466	2.456	0.38	
			0.562	1.128	1.758	2.427	2.466				
iba RAZOR^{Chamber} SN 16294	1112	130	0.484	1.010	1.581	2.252	2.288	2.289	2.456	-6.79	
			0.485	1.101	1.584	2.255	2.291				
iba RAZOR$^{Nano\ Chamber}$ SN 16233	1113	130	0.403	0.802	1.270	1.829	1.858	2.068	2.456	-15.81	
			0.488	0.967	1.493	2.047	2.079				
			0.486	0.958	1.480	2.024	2.056				
iba RAZOR$^{Diode\ Detector}$ SN 10581	1104	130	0.5959	1.1724	1.7954	2.4298	2.4684	2.473	2.456	0.71	
			0.597	1.174	1.797	2.440	2.479				
			2.975E-09	5.853E-09	8.963E-09	1.213E-08	1.232E-08		[C]		
			2.979E-09	5.860E-09	8.969E-09	1.218E-08	1.237E-08				
PTW microDiamond SN 123497 (UNIDOS (A))	1104	130	0.640	1.232	1.833	2.421	2.459	2.458	2.456	0.09	
			0.641	1.231	1.831	2.419	2.457				
PTW microDiamond SN 123497 (Dose²)	1104	130	0.632	1.200	1.838	2.445	2.484	2.485	2.456	1.19	
			0.635	1.199	1.840	2.448	2.487				
PTW 0.3 cm³ Semiflex Chamber SN 0190 (UNIDOS (A))	1107	130	0.545	1.099	1.700	2.349	2.424	2.424	2.456	-1.31	N4 correction with P_{TP} and $N_{D,W}$
			0.544	1.092	1.700	2.348	2.423				

	Date	[]	09.04.2021
Plan	Source aktivity	[Ci]	4.68
Plan	Total traeatment time	[s]	9880
	Method	[]	Timed continuous
	Range	[]	iba Low PTW High
	Length	[mm]	see Table
	Air pressure	[hPa]	1003.3
	Temperature	[°C]	21.8
	P_{TP}	[]	1.02
	For 0.3 cm³ Semiflex Chamber		
	$N_{D,W}$	[]	1.016

	All CC's [Gy]	RAZOR Diode Detector [C]	Calibration factor [Gy/C]
Mean	2.473	1.235E-08	2.0032E+08
Planning	2.456		
Relative Derivation	0.71%		

Treatment plan			Ion chamber		
OMP Plan		see Table	Manufacturer	-	
TCC Plan		NORM_4Nadeln HDR	Model	see Table	
Phantom		Needle	SN	-	
Source calibration data			Electrometer		
Date		07.01.2021	Manufacturer	iba	PTW
Aktivity [Ci]		11.10	Model	Dose²	UNIDOS (A)
SN		NLF01D85E5930	SN	00298	10273

OMP		Measurement range		Step size	Time per position	N1	N2	N3	N4	N4 correction with p_{TP}	Planning	Deviation	
		[mm]	[mm]	[mm]	[s]	[Gy]	[Gy]	[Gy]	[Gy]	[Gy]	[Gy]	[%]	
iba CC04	SN 16286	1086	1134	4	12	0.647	1.252	1.875	2.482	2.521	2.530	-0.35	
iba CC13	SN 16296	1087	1135	4	12	0.593	1.188	1.838	2.522	2.562	2.530	1.26	
iba CC25	SN 16125	1089	1137	4	12	0.586	1.175	1.822	2.503	2.543	2.530	0.49	
iba RAZOR^{Chamber}	SN 16294	1088	1136	4	12	0.500	1.024	1.617	2.285	2.321	2.530	-8.26	
iba RAZOR$^{Nano\ Chamber}$	SN 16233	1089	1137	4	12	0.487	0.964	1.482	2.014	2.046	2.530	-19.14	
iba RAZOR$^{Diode\ Detector}$	SN 10581	1080	1128	4	12	0.635	1.250	1.903	2.566	2.607	2.530	3.03	correcton whit calibration coefficient 2,0032E+08
						3.17E-09	6.24E-09	9.50E-09	1.28E-08		[C]		
PTW microDiamond (UNIDOS (A))	SN 123496	1080	1128	4	12	0.658	1.256	1.878	2.482	2.521	2.530	-0.35	
PTW microDiamond (DOSE²)	SN 123496	1080	1128	4	12	0.644	1.233	1.890	2.513	2.553	2.530	0.90	
PTW 0.3 cm³ Semiflex Chamber	SN 0190	1083	1131	4	10	0.475	0.947	1.479	2.033	2.098	2.108	-0.47	N4 correction with P_{TP} and $N_{D,W}$

	Date	[]	09.04.2021
Plan	Source aktivity	[Ci]	4.68
Plan	Total traeatment time	[s]	5512
	Method	[]	Timed continuous
	Range	[]	iba Low PTW High
	Length	[mm]	see Table
	Air pressure	[hPa]	1003.3
	Temperature	[°C]	21.8
	P_{TP}	[]	1.02
	For 0.3 cm³ Semiflex Chamber		
	$N_{D,W}$	[]	1.016

C Water phantom Data

Table 22: Overview of the project procedure for the water phantom. The values in the table stand for the measurement days, the year was omitted.

Treatment	CC04	CC13	CC25	RAZOR Chamber	RAZOR Nano	RAZOR Diode	micro-Diamond	0.3 cm^3 Semiflex
max. Signal	14.04. 22.04.	07.04. 25.04. 26.04.	08.04. 14.04. 22.04. 23.04.	21.04.	15.04.	29.04.	25.02. 12.03. 16.03. - 18.03. 25.03.	08.04.
Dose linearity of point-source	14.04.	26.03.	08.04.	21.04.	15.04.		25.02.	
Point-source - depth dose	14.04.	25.03.	08.04.	21.04.	16.04.		11.03. 16.03. 17.03.	
Point-source - cross profile		26.03.	08.04.				11.03. 12.03.	
3 cm active length - depth dose	15.04.	26.03.	08.04.	21.04.	16.04.		12.03. 16.03.	
3 cm active length - cross profile		26.03.					12.03. 18.03	
5 cm active length - depth dose	15.04.	26.03. 16.04.	08.04. 22.04. 23.04.	21.04.	15.04.	29.04.	12.03.	
5 cm active length - cross profile	22.04.	26.03.	22.04.				18.03.	
8 cm active length - depth dose	14.04.	26.03.	14.04.	21.04.	16.04.		16.03. 17.03.	
8 cm active length - cross profile		26.03.					17.03.	
12 cm active length - depth dose	14.04.	07.04.	14.04.	21.04.	16.04.		17.03.	
12 cm active length - cross profile		07.04.					18.03.	
5 needles in triangular configuration	15.04. 28.04.	07.04.	14.03. 23.04.	21.04.	16.04.		25.03.	
Dependance on water heights		16.04.			16.04.			
Number of measurements(n)	155	304	203	96	109	73	642	59

Treatment plan	
OMP Plan	OMP_1Nadel-Pkt
TCC Plan	Nadel PTW HDR
Phantom	PTW water Phantom
Source calibration data	
Date	02.03.2021
Aktivity [Ci]	12.48
SN	NLF01D85E6191

Summary point-source - depth dose in the water phantom

SD = Standard derivation

Ion chamber									
Manufacturer	iba	iba	iba	iba	iba	PTW	PTW	PTW	PTW
Model	CC04	CC13	CC25	RAZOR[Chamber]	RAZOR[Nano Chamber]	microDiamond	microDiamond	microDiamond	microDiamond
SN	16286	16296	16125	16294	16233	123497	123497	123497	123497
Electrometer									
Manufacturer	iba	iba	iba	iba	iba	PTW	PTW	PTW	PTW
Model	Dose²	Dose²	Dose²	Dose²	Dose²	UNIDOSE (A)	Dose²	Dose²	Dose²
SN	00298	00298	00298	00298	00298	10273	00298	00298	00298

A-Axis coordinates [mm]	CC04 Mean correction with p_{TP} [Gy]	CC04 Planning [Gy]	CC04 Deviation [%]	CC13 Mean correction with p_{TP} [Gy]	CC13 Planning [Gy]	CC13 Deviation [%]	CC25 Mean correction with p_{TP} [Gy]	CC25 Planning [Gy]	CC25 Deviation [%]	RAZOR[Chamber] Mean correction with p_{TP} [Gy]	RAZOR[Chamber] Planning [Gy]	RAZOR[Chamber] Deviation [%]
5												
10												
15	7.250	7.047	2.88				2.568	2.490	3.15	7.166	6.614	6.08
20	4.180	3.980	5.04	4.692	4.800	-2.24	4.393	4.219	4.12	4.071	3.735	9.00
25	2.663	2.552	4.34	3.042	3.079	-1.20	2.886	2.706	6.66	2.589	2.396	8.09
30	1.836	1.774	3.49	2.161	2.139	1.03	1.960	1.880	4.26	1.784	1.665	7.19
35	1.345	1.303	3.25	1.608	1.571	2.36	1.474	1.381	6.75	1.314	1.223	7.42
40	1.023	0.997	2.70	1.217	1.202	1.28	1.122	1.056	6.21	0.995	0.935	6.34
45	0.805	0.786	2.47	0.961	0.948	1.42	0.885	0.833	6.18	0.776	0.738	5.23
50	0.647	0.635	1.95	0.776	0.766	1.37	0.712	0.673	5.86	0.620	0.596	4.11
Mean			3.27			0.57			5.40			6.68
SD			0.95			1.52			1.27			1.47
Min.			1.95			-2.24			3.15			4.11
Max.			5.04			2.36			6.75			9.00

A-Axis coordinates [mm]	RAZOR[Nano Chamber] Mean correction with p_{TP} [Gy]	RAZOR[Nano Chamber] Planning [Gy]	RAZOR[Nano Chamber] Deviation [%]	microDiamond (UNIDOSE) Mean correction with p_{TP} [Gy]	Planning [Gy]	Deviation [%]	microDiamond Mean correction with p_{TP} [Gy]	Planning [Gy]	Deviation [%]	microDiamond Mean correction with p_{TP} [Gy]	Planning [Gy]	Deviation [%]	microDiamond Mean correction with p_{TP} [Gy]	Planning [Gy]	Deviation [%]
5				3.946	3.355	17.63	20.077	16.004	25.45				20.455	15.873	28.87
10				1.629	1.444	12.86	4.694	4.132	13.59	4.698	4.132	13.70	4.696	4.098	14.58
15	7.441	6.932	7.34	1.406	1.293	8.74	2.006	1.850	8.42	2.032	1.850	9.85	2.020	1.835	10.10
20	4.217	3.915	7.73	1.559	1.460	6.77	1.095	1.045	4.80	1.121	1.045	7.29	1.114	1.036	7.55
25	2.645	2.511	5.34	1.481	1.404	5.45	0.684	0.670	2.06	0.711	0.670	6.05	0.707	0.665	6.33
30	1.748	1.745	0.20	1.529	1.464	4.43	0.462	0.466	-0.84	0.490	0.466	5.28	0.486	0.462	5.15
35	1.301	1.282	1.48	1.491	1.434	3.95	0.330	0.342	-3.62	0.358	0.342	4.54	0.355	0.339	4.72
40	0.976	0.980	-0.44				0.246	0.262	-5.94	0.272	0.262	4.14	0.270	0.259	4.05
45	0.757	0.773	-2.12				0.186	0.206	-9.67	0.214	0.206	3.64	0.212	0.205	3.79
50	0.598	0.625	-4.23				0.143	0.167	-14.36	0.172	0.167	3.30	0.171	0.165	3.71
Mean			1.91			**8.55**			1.99			6.42			**8.89**
SD			4.15			**4.66**			11.14			3.22			**7.41**
Min.			-4.23			**3.95**			-14.36			3.30			**3.71**
Max.			7.73			**17.63**			25.45			13.70			**28.87**

		CC04	CC13	CC25	RAZOR[Chamber]	RAZOR[Nano Chamber]	microDiamond	microDiamond	microDiamond	microDiamond
Date	[]	14.04.2021	25.03.2021	08.04.2021	21.04.2021	16.04.2021	11.03.2021	16.03.2021	16.03.2021	17.03.2021
Plan: Source aktivity	[Ci]	8.33	10.06	8.82	7.80	8.18	11.47	10.94	10.94	10.84
Plan: Total traeatment time	[s]	1200	2100	2200	670	1200	2434	600	600	600
Method	[]	Timed collection see Table	Timed collection see Table	Timed collection see Table	Timed collection see Table	Timed collection see Table	Timed collection see Table	Timed collection see Table	Timed collection see Table	Timed collection see Table
Range	[]	Low	Low	Low	Low	Low	High	High	Low	Low
Length	[mm]	1132	1132	1129	1129	1129	1090	1119	1119	1120
Air pressure	[hPa]	1002.5	999.4	1003.4	1001.9	1001.5	988.8	995.7	995.7	997.1
Temperature	[°C]	21.4	22.2	22.1	21.3	21.1	21.4	21.4	21.4	21.3
P_{TP}	[]	1.02	1.02	1.02	1.02	1.02	1.03	1.02	1.02	1.02

A-Axis coordinates [mm]	CC04 Normalised whit 20 mm [%]	CC04 Planning [%]	CC04 Deviation of normalised data [%]	CC13 Normalised whit 20 mm [Gy]	CC13 Planning [%]	CC13 Deviation of normalised data [%]	CC25 Normalised whit 20 mm [%]	CC25 Planning [%]	CC25 Deviation of normalised data [%]	RAZOR[Chamber] Normalised whit 20 mm [%]	RAZOR[Chamber] Planning [%]	RAZOR[Chamber] Deviation of normalised data [%]
5												
10												
15	173.5	177.1	3.63				58.5	59.0	0.55	176.0	177.1	1.06
20	100.0	100.0	0.00	100.0	100.0	0.00	100.0	100.0	0.00	100.0	100.0	0.00
25	63.7	64.1	0.43	64.8	64.1	-0.69	65.7	64.1	-1.56	63.6	64.1	0.54
30	43.9	44.6	0.65	46.1	44.6	-1.49	44.6	44.6	-0.06	43.8	44.6	0.74
35	32.2	32.7	0.56	34.3	32.7	-1.54	33.6	32.7	-0.83	32.3	32.7	0.47
40	24.5	25.0	0.56	25.9	25.0	-0.90	25.5	25.0	-0.50	24.4	25.0	0.61
45	19.3	19.7	0.48	20.5	19.7	-0.74	20.1	19.7	-0.39	19.1	19.7	0.68
50	15.5	16.0	0.47	16.5	16.0	-0.59	16.2	16.0	-0.27	15.2	16.0	0.72
Mean			0.85			-0.85			-0.38			0.60
SD			1.07			0.50			0.58			0.28
Min.			0.00			-1.54			-1.56			0.00
Max.			3.63			0.00			0.55			1.06

A-Axis coordinates [mm]	RAZOR[Nano Chamber] Normalised whit 20 mm [%]	RAZOR[Nano Chamber] Planning [%]	RAZOR[Nano Chamber] Deviation of normalised data [%]	microDiamond Normalised whit 20 mm [%]	microDiamond Planning [%]	microDiamond Absolute Deviation [%]	microDiamond Normalised whit 20 mm [%]	Planning [%]	Deviation of normalised data [%]	microDiamond Normalised whit 20 mm [%]	Planning [%]	Deviation of normalised data [%]	microDiamond Normalised whit 20 mm [%]	Planning [%]	Deviation of normalised data [%]
5							1833.8	1531.9	-301.91				1835.6	1532.0	-303.66
10							428.7	395.5	-33.19	419.2	395.5	-23.63	421.4	395.5	-25.84
15	176.4	177.1	0.64				183.2	177.1	-6.12	181.3	177.1	-4.23	181.3	177.1	-4.20
20	100.0	100.0	0.00				100.0	100.0	0.00	100.0	100.0	0.00	100.0	100.0	0.00
25	62.7	64.1	1.42				62.5	64.1	1.67	63.4	64.1	0.74	63.4	64.1	0.73
30	41.5	44.6	3.12				42.2	44.6	2.40	43.7	44.6	0.84	43.6	44.6	0.99
35	30.8	32.7	1.90				30.1	32.7	2.63	31.9	32.7	0.84	31.9	32.7	0.86
40	23.1	25.0	1.90				22.5	25.0	2.57	24.3	25.0	0.74	24.2	25.0	0.81
45	17.9	19.7	1.81				17.0	19.7	2.73	19.1	19.7	0.67	19.1	19.7	0.69
50	14.2	16.0	1.77				13.0	16.0	2.92	15.4	16.0	0.59	15.4	16.0	0.57
Mean			1.57	Note: Different times in the measurement therefore not comparabl with the other results.					-32.63			-2.60			**-32.90**
SD			0.87						90.38			7.59			**90.59**
Min.			0.00						-301.91			-23.63			**-303.66**
Max.			3.12						2.92			0.84			**0.99**

Summary depth-dose - Length (3, 5, 8, 12 cm) in the water phantom

MS = Measurement series OMP = Oncentra Masterplan
SD = Standard derivation

Treatment plan		Ion chamber								
OMP Plan	see Table	Manufacturer	iba	iba	iba	iba	iba	iba	PTW	PTW
TCC Plan	Nadel PTW HDR	Model	CC04	CC13	CC25	RAZOR Chamber	RAZOR Nano Chamber	RAZOR Diode Detector	microDiamond	microDiamond
Phantom	PTW water Phantom	SN	16286	16296	16125	16294	16233	10581	123497	123497
Source calibration data		Electrometer								
Date	02.03.2021	Manufacturer	iba	iba	iba	iba	iba	iba	PTW	iba
Aktivity [Ci]	12.48	Model	Dose²	Dose²	Dose²	Dose²	Dose²	Dose²	UNIDOSE (A)	Dose²
SN	NLF01D85E6191	SN	00298	00298	00298	00298	00298	00298	10273	00298

Column groups of the main table, by detector (MS correction with p_{TP} [Gy] / Planning [Gy] / Deviation [%]): CC04 | CC13 | CC25 | RAZOR Chamber | RAZOR Nano Chamber | RAZOR Diode Detector | microDiamond (UNIDOSE) | microDiamond (Dose²)

OMP	A-Axis coordinates [mm]	MS correction with p_{TP} [Gy]	Planning [Gy]	Deviation [%]	MS correction with p_{TP} [Gy]	Planning [Gy]	Deviation [%]	MS correction with p_{TP} [Gy]	Planning [Gy]	Deviation [%]
OMP_1Nadel-3cm	5									
	10									
	15	9.883	9.613	2.81	1.806	1.855	-2.66	6.491	6.153	5.51
	20	6.311	6.015	4.93	1.139	1.161	-1.84	4.120	3.850	7.02
	25	4.270	4.086	4.49	0.794	0.789	0.73	2.794	2.615	6.84
	30	3.057	2.942	3.91	0.572	0.568	0.75	2.003	1.883	6.38
	35	2.285	2.212	3.32	0.432	0.427	1.31	1.503	1.415	6.18
	40	1.768	1.718	2.87	0.336	0.332	1.25	1.165	1.100	5.95
	45	1.407	1.370	2.67	0.268	0.264	1.39	0.929	0.877	5.98
	50	1.136	1.116	1.82	0.219	0.215	1.60	0.755	0.714	5.70
Mean				3.35			0.32			6.19
SD				0.91			1.43			0.47
Min.				1.82			-2.66			5.51
Max.				4.93			1.60			7.02
OMP_1Nadel-5cm	15	5.413	5.352	1.13	5.363	5.294	1.30	5.909	5.921	-0.19
	16	5.015	4.898	2.40	4.977	4.844	2.75	5.450	5.418	0.59
	17	4.640	4.499	3.14	4.584	4.450	3.01	5.010	4.977	0.67
	18	4.304	4.147	3.79	4.242	4.102	3.42	4.605	4.588	0.37
	19	3.974	3.835	3.62	3.908	3.793	3.04	4.255	4.242	0.31
	20	3.678	3.556	3.41	3.625	3.518	3.05	3.934	3.934	0.01
	21	3.417	3.306	3.34	3.374	3.270	3.18	3.643	3.658	-0.40
	22	3.181	3.082	3.21	3.146	3.048	3.21	3.386	3.409	-0.66
	23	2.971	2.878	3.20	2.934	2.847	3.06	3.154	3.184	-0.94
	24	2.786	2.694	3.41	2.740	2.665	2.81	2.942	2.980	-1.27
	25	2.614	2.527	3.43	2.568	2.499	2.76	2.754	2.795	-1.46
	26	2.407	2.374	1.40	2.409	2.348	2.63	2.582	2.626	-1.67
	28	2.162	2.150	0.55	2.139	2.083	2.70	2.282	2.329	-2.00
	30	1.932	1.879	2.82	1.904	1.859	2.44	2.021	2.079	-2.79
Mean				2.78			2.81			-0.67
SD				0.98			0.49			1.02
Min.				0.55			1.30			-2.79
Max.				3.79			3.42			0.67
OMP_1Nadel-5cm	5									
	10									
	15	5.413	5.352	1.13	3.418	3.518	-2.84	5.479	5.190	5.56
	20	3.678	3.556	3.41	2.337	2.338	-0.04	3.697	3.449	7.21
	25	2.614	2.527	3.45	1.671	1.661	0.58	2.610	2.450	6.54
	30	1.932	1.879	2.82	1.238	1.235	0.24	1.932	1.822	6.03
	35	1.488	1.447	2.83	0.959	0.951	0.81	1.482	1.403	5.66
	40	1.170	1.145	2.26	0.757	0.752	0.67	1.171	1.110	5.55
	45	0.944	0.925	2.02	0.613	0.608	0.80	0.944	0.897	5.24
	50	0.772	0.761	1.42	0.504	0.500	0.76	0.776	0.738	5.17
	60							1.102	1.089	1.24
	70							0.808	0.804	0.50
	80							0.612	0.614	-0.24
	90							0.949	0.962	-1.33
	100							0.753	0.769	-2.09
	120							0.740	0.771	-4.03
	140							0.703	0.748	**-6.04**
	160							0.643	0.702	-8.37
	180							0.462	0.518	-10.92
	200							0.391	0.449	-12.75
Mean				2.42			0.12			0.16
SD				0.76			1.09			6.20
Min.				1.13			-2.84			-12.75
Max.				3.45			0.81			7.21
OMP_1Nadel-8cm	5									
	10									
	15	7.238	7.141	1.36	2.449	2.507	-2.30	7.390	7.141	3.49
	20	5.094	4.964	2.61	1.748	1.743	0.31	5.174	4.964	4.23
	25	3.757	3.761	-0.12	1.295	1.289	0.51	3.805	3.761	1.16
	30	2.872	2.825	1.67	0.996	0.992	0.46	2.913	2.825	3.12
	35	2.273	2.238	1.58	0.790	0.786	0.62	2.294	2.238	2.50
	40	1.829	1.812	0.92	0.640	0.636	0.59	1.853	1.812	2.28
	45	1.504	1.493	0.73	0.528	0.524	0.67	1.524	1.493	2.10
	50	1.252	1.248	0.34	0.441	0.438	0.72	1.266	1.248	1.49
Mean				1.14			0.20			2.54
SD				0.75			0.90			0.91
Min.				-0.12			-2.30			1.16
Max.				2.61			0.72			4.23

OMP	A-Axis coordinates [mm]	MS correction with p_{TP} [Gy]	Planning [Gy]	Deviation [%]	MS correction with p_{TP} [Gy]	Planning [Gy]	Deviation [%]	MS correction with p_{TP} [Gy]	Planning [Gy]	Deviation [%]
OMP_1Nadel-3cm	5									
	10									
	15	9.95	9.98	-0.23	9.997	9.534	4.86			
	20	6.23	5.68	9.76	6.262	5.966	4.97			
	25	4.17	3.86	8.01	4.204	4.053	3.74			
	30	2.96	2.78	6.60	2.970	2.918	1.78			
	35	2.21	2.09	5.75	2.202	2.194	0.39			
	40	1.70	1.62	4.50	1.673	1.704	-1.83			
	45	1.34	1.29	3.35	1.314	1.359	-3.32			
	50	1.08	1.05	2.29	1.049	1.107	-5.22			
Mean				5.00			0.67			
SD				2.84			3.39			
Min.				-0.23			-5.22			
Max.				9.76			4.97			
OMP_1Nadel-5cm	15	6.047	5.525	9.44	5.473	5.352	2.26	4.419	4.244	4.13
	16	5.590	5.056	10.55	5.065	4.898	3.41	3.681	3.468	6.16
	17	5.148	4.644	10.85	4.574	4.499	1.67	3.085	2.911	6.00
	18	4.744	4.281	10.81	4.280	4.147	3.19	2.691	2.492	8.02
	19	4.366	3.959	10.29	3.972	3.835	3.58	2.341	2.166	8.08
	20	4.076	3.671	11.02	3.661	3.556	2.95	2.058	1.906	7.97
	21	3.773	3.413	10.53	3.393	3.306	2.62	1.828	1.693	7.95
	22	3.512	3.181	10.41	3.143	3.082	2.00	1.643	1.516	8.40
	23	3.261	2.972	9.74	2.933	2.878	1.89	1.479	1.366	8.26
	24	3.045	2.781	9.50	2.750	2.694	2.08	1.349	1.239	8.94
	25	2.845	2.608	9.09	2.558	2.527	1.24	1.232	1.128	9.17
	26	2.661	2.450	8.62	2.414	2.374	1.71	2.253	2.065	9.12
	28	2.352	2.174	8.21	2.122	2.150	-1.34	2.070	1.897	9.11
	30	2.091	1.940	7.77	1.872	1.879	-0.39	1.912	1.749	9.35
Mean				9.77			1.92			7.90
SD				1.00			1.33			1.44
Min.				7.77			-1.34			4.13
Max.				11.02			3.58			9.35
OMP_1Nadel-5cm	5							4.42	4.24	**4.13**
	10							2.06	1.91	**7.97**
	15	6.05	5.53	9.44	5.473	5.352	2.26	1.23	1.13	**9.17**
	20	4.08	3.67	11.02	3.661	3.556	2.95	1.66	1.50	10.47
	25	2.85	2.61	9.09	2.558	2.527	1.25	1.20	1.07	12.92
	30	2.09	1.94	7.77	1.872	1.879	-0.39	2.70	2.38	13.66
	35	1.59	1.49	6.39	1.427	1.447	-1.38	2.12	1.83	16.07
	40	1.24	1.18	5.20	1.105	1.145	-3.46	1.71	1.45	18.05
	45	0.99	0.95	3.79	0.877	0.925	-5.20	1.41	1.17	20.62
	50	0.80	0.79	2.49	0.708	0.761	-6.92	1.19	0.96	23.59
	60									
	70									
	80									
	90									
	100									
	120									
	140									
	160									
	180									
	200									
Mean				6.90			-1.36			13.66
SD				2.61			3.15			5.45
Min.				2.49			-6.92			4.13
Max.				11.02			2.95			23.59
OMP_1Nadel-8cm	5									
	10									
	15	7.05	6.68	5.56	7.184	7.011	2.47			
	20	4.91	4.64	5.76	5.000	4.874	2.60			
	25	3.59	3.43	4.47	3.635	3.604	0.85			
	30	2.74	2.64	3.63	2.751	2.774	-0.80			
	35	2.15	2.09	2.67	2.141	2.197	-2.54			
	40	1.72	1.69	1.55	1.701	1.779	-4.40			
	45	1.40	1.40	0.59	1.378	1.466	-5.99			
	50	1.16	1.17	-0.39	1.129	1.225	-7.82			
Mean				2.98			-1.95			
SD				2.01			3.44			
Min.				-0.39			-7.82			
Max.				5.76			2.60			

OMP	A-Axis coordinates [mm]	MS correction with p_{TP} [Gy]	Planning [Gy]	Deviation [%]	MS correction with p_{TP} [Gy]	Planning [Gy]	Deviation [%]
OMP_1Nadel-3cm	5	12.540	11.741	**6.80**	12.471	11.277	**10.59**
	10	5.120	4.833	**5.95**	4.969	4.642	**7.05**
	15	2.770	2.647	**4.67**	2.699	2.542	**6.15**
	20	1.734	1.656	4.69	1.679	1.591	5.51
	25	1.170	1.125	3.98	1.138	1.081	5.28
	30	0.842	0.810	4.00	0.817	0.778	5.02
	35	0.632	0.609	3.80	0.613	0.585	4.76
	40	0.488	0.473	3.16	0.474	0.455	4.34
	45	0.389	0.377	3.08	0.378	0.362	4.45
	50	0.316	0.307	2.93	0.307	0.295	4.16
Mean				4.31			5.73
SD				1.14			1.74
Min.				2.93			4.16
Max.				6.80			10.59
OMP_1Nadel-5cm	15–30						
Mean							
SD							
Min.							
Max.							
OMP_1Nadel-5cm	5	13.114	12.690	**3.34**			
	10	5.788	5.698	**1.57**			
	15	3.379	3.374	**0.16**			
	20	2.244	2.242	0.11			
	25	1.591	1.593	-0.09			
	30	1.186	1.185	0.14			
	35	0.913	0.912	0.08			
	40	0.719	0.722	-0.35			
	45	0.582	0.583	-0.12			
	50	0.478	0.480	-0.40			
Mean				0.44			
SD				1.05			
Min.				-0.40			
Max.				3.34			
OMP_1Nadel-8cm	5				10.774	9.420	**14.38**
	10				4.808	4.432	**8.48**
	15				2.933	2.753	**6.52**
	20				2.014	1.914	5.21
	25				1.478	1.416	4.43
	30				1.138	1.089	4.45
	35				0.896	0.863	3.86
	40				0.724	0.699	3.61
	45				0.597	0.576	3.64
	50				0.497	0.481	3.41
Mean							5.80
SD							3.08
Min.							3.41
Max.							14.38

OMP_1Nadel-12cm	5																						11.287	9.521	18.55
	10																						5.061	4.593	10.19
	15	5.878	5.874	0.07	2.259	2.413	-6.36	6.009	5.874	2.30	5.66	5.49	3.09	5.759	5.765	-0.10							3.165	2.933	7.91
	20	4.257	4.200	1.37	1.669	1.725	-3.24	4.344	4.200	3.43	4.07	3.93	3.76	4.112	4.122	-0.23							2.231	2.097	6.39
	25	3.232	3.191	1.28	1.282	1.311	-2.19	3.287	3.191	3.00	3.06	2.98	2.43	3.070	3.132	-1.96							1.681	1.593	5.50
	30	2.535	2.519	0.63	1.011	1.035	-2.26	2.579	2.519	2.37	2.39	2.36	1.55	2.368	2.473	-4.24							1.323	1.258	5.14
	35	2.053	2.044	0.46	0.823	0.839	-1.95	2.087	2.044	2.10	1.92	1.91	0.55	1.895	2.006	-5.54							1.071	1.020	4.92
	40	1.689	1.690	-0.06	0.682	0.694	-1.84	1.717	1.690	1.57	1.57	1.58	-0.48	1.537	1.659	-7.34							0.883	0.844	4.61
	45	1.419	1.419	0.00	0.573	0.583	-1.73	1.437	1.419	1.22	1.31	1.33	-1.41	1.271	1.393	-8.74							0.741	0.709	4.49
	50	1.200	1.207	-0.53	0.489	0.496	-1.42	1.219	1.207	1.07	1.10	1.13	-2.13	1.059	1.184	-10.57							0.630	0.602	4.51
Mean				0.40			-2.62			2.13			0.92			-4.84									7.22
SD				0.59			1.41			0.73			1.89			3.45									3.96
Min.				-0.53			-6.36			1.07			-2.13			-10.57									4.49
Max.				1.37			-1.42			3.43			3.76			-0.10									18.55
Over all measured values	Mean			**2.12**			**0.51**			**1.44**			**5.72**			**-0.72**			**10.30**			**2.37**			**6.25**
	SD			**1.36**			**2.15**			**4.24**			**3.92**			**3.89**			**4.78**			**2.25**			**3.29**
	Min.			**-0.53**			**-6.36**			**-12.75**			**-2.13**			**-10.57**			**4.13**			**-0.40**			**3.41**
	Max.			**4.93**			**3.42**			**7.21**			**11.02**			**4.97**			**23.59**			**6.80**			**18.55**

	Date	[]	15.04.2021	07.04.2021	08.04.2021	21.04.2021	16.04.2021	29.04.2021	12.03.2021	17.03.2021
Plan	Source aktivity	[Ci]	8.26	8.90	8.82	7.80	8.18	3.88	11.36	10.84
Plan	Total traeatment time	[s]	10516	3296	2760	16056	8280	3330	1230	3150
	Method	[]	Timed continuous	Timed continuous	Timed continuous	Timed continuous	Timed continuous	Timed continuous	Timed continuous	Timed continuous
	Range	[]	Low	Low	Low	Low	Low	Low	High	High
	Length	[mm]	see Table	see Table	see Table	see Table	see Table	see Table	see Table	see Table
	Air pressure	[hPa]	1002.9	992.2	1003.4	995.6	1001.5	987.4	992.7	997
	Temperature	[°C]	21.2	22.5	22.1	21.1	21.1	21.4	21.4	21.3
	P_{TP}	[]	1.01	1.03	1.02	1.02	1.02	1.03	1.03	1.02

		CC04			CC13			CC25			RAZOR[Chamber]			RAZOR[Nano Chamber]			RAZOR[Diode Detector]			microDiamond			microDiamond		
OMP	A-Axis coordinates [mm]	Normalised whit 20 mm [%]	Planning [%]	Deviation of normalised data [%]	Normalised whit 20 mm [%]	Planning [%]	Deviation of normalised data [%]	Normalised whit 20 mm [%]	Planning [%]	Deviation of normalised data [%]	Normalised whit 20 mm [%]	Planning [%]	Deviation of normalised data [%]	Normalised whit 20 mm [%]	Planning [%]	Deviation of normalised data [%]	Normalised whit 20 mm [%]	Planning [%]	Deviation of normalised data [%]	Normalised whit 20 mm [%]	Planning [%]	Deviation of normalised data [%]	Normalised whit 20 mm [%]	Planning [%]	Deviation of normalised data [%]
OMP_1Nadel-3cm	5																			723.2	708.9	-14.34	743.0	708.9	-34.11
	10																			295.3	291.8	-3.52	296.0	291.8	-4.24
	15	156.6	159.8	3.22	158.5	159.8	1.34	157.6	159.8	2.26	159.7	175.7	15.99	159.6	159.8	0.17				159.8	159.8	0.03	160.8	159.8	-0.97
	20	100.0	100.0	0.00	100.0	100.0	0.00	100.0	100.0	0.00	100.0	100.0	0.00	100.0	100.0	0.00				100.0	100.0	0.00	100.0	100.0	0.00
	25	67.7	67.9	0.28	69.7	67.9	-1.78	67.8	67.9	0.12	66.9	67.9	1.08	67.1	67.9	0.80				67.5	67.9	0.46	67.8	67.9	0.15
	30	48.4	48.9	0.48	50.2	48.9	-1.29	48.6	48.9	0.29	47.5	48.9	1.41	47.4	48.9	1.49				48.6	48.9	0.32	48.7	48.9	0.23
	35	36.2	36.8	0.56	37.9	36.8	-1.18	36.5	36.8	0.29	35.4	36.8	1.34	35.2	36.8	1.60				36.5	36.8	0.31	36.5	36.8	0.26
	40	28.0	28.6	0.56	29.5	28.6	-0.90	28.3	28.6	0.29	27.2	28.6	1.37	26.7	28.6	1.85				28.1	28.6	0.42	28.3	28.6	0.32
	45	22.3	22.8	0.49	23.5	22.8	-0.75	22.6	22.8	0.22	21.4	22.8	1.33	21.0	22.8	1.80				22.4	22.8	0.35	22.5	22.8	0.23
	50	18.0	18.5	0.55	19.2	18.5	-0.65	18.3	18.5	0.23	17.3	18.5	1.26	16.7	18.5	1.80				18.2	18.5	0.31	18.3	18.5	0.24
Mean				0.77			-0.65			0.46			2.97			1.19						-1.57			-3.79
SD				0.89			0.84			0.65			4.66			0.67						4.20			9.72
Min.				0.00			-1.78			0.00			0.00			0.00						-14.34			-34.11
Max.				3.22			1.34			2.26			15.99			1.85						0.46			0.32
OMP_1Nadel-5cm	15	147.2	150.5	3.31	148.0	150.5	2.55	150.2	150.5	0.31	148.4	150.5	2.14	149.5	150.5	1.014	214.8	222.7	7.92						
	16	136.4	137.7	1.34	137.3	137.7	0.40	138.5	137.7	-0.80	137.1	137.7	0.58	138.3	137.7	-0.618	178.9	182.0	3.05						
	17	126.2	126.5	0.33	126.5	126.5	0.04	127.3	126.5	-0.83	126.3	126.5	0.19	124.9	126.5	1.568	149.9	152.7	2.79						
	18	117.0	116.6	-0.43	117.0	116.6	-0.42	117.0	116.6	-0.42	116.4	116.6	0.23	116.9	116.6	-0.277	130.8	130.7	-0.07						
	19	108.1	107.8	-0.22	107.8	107.8	0.00	108.2	107.8	-0.32	107.1	107.8	0.72	108.5	107.8	-0.657	113.8	113.7	-0.12						
	20	100.0	100.0	0.00	100.0	100.0	0.00	100.0	100.0	0.00	100.0	100.0	0.00	100.0	100.0	0.000	100.0	100.0	0.00						
	21	92.9	93.0	0.06	93.1	93.0	-0.12	92.6	93.0	0.38	92.6	93.0	0.42	92.7	93.0	0.299	88.8	88.8	0.02						
	22	86.5	86.7	0.16	86.8	86.6	-0.13	86.1	86.7	0.58	86.2	86.7	0.48	85.9	86.7	0.798	79.9	79.5	-0.32						
	23	80.8	80.9	0.16	80.9	80.9	-0.01	80.2	80.9	0.77	80.0	80.9	0.94	80.1	80.9	0.829	71.9	71.7	-0.19						
	24	75.8	75.8	0.00	75.6	75.8	0.17	74.8	75.8	0.97	74.7	75.8	1.04	75.1	75.8	0.643	65.6	65.0	-0.59						
	25	71.1	71.1	-0.01	70.8	71.0	0.19	70.0	71.0	1.05	69.8	71.0	1.24	69.9	71.1	1.181	59.9	59.2	-0.66						
	26	65.4	66.7	1.30	66.5	66.7	0.27	65.6	66.7	1.12	65.3	66.7	1.45	65.9	66.7	0.806	109.5	108.4	-1.15						
	28	58.8	60.5	1.67	59.0	59.2	0.20	58.0	59.2	1.19	57.7	59.2	1.50	57.9	60.5	2.522	100.6	99.5	-1.06						
	30	52.5	52.8	0.30	52.5	52.8	0.31	51.4	52.8	1.48	51.3	52.8	1.55	51.1	52.8	1.714	92.9	91.8	-1.17						
Mean				0.57			0.25			0.39			0.89			0.70			0.60						
SD				0.97			0.67			0.73			0.60			0.87			2.38						
Min.				-0.43			-0.42			-0.83			0.00			-0.66			-1.17						
Max.				3.31			2.55			1.48			2.14			2.52			7.92						
OMP_1Nadel-5cm	5																266.8	283.0	16.24	584.3	566.0	-18.25			
	10																124.2	127.1	2.87	257.9	254.2	-3.72			
	15	147.2	150.5	3.31	146.3	150.5	4.22	148.2	150.5	2.32	148.4	150.5	2.14	149.5	150.5	1.01	74.4	75.2	0.88	150.6	150.5	-0.07			
	20	100.0	100.0	0.00	100.0	100.0	0.00	100.0	100.0	0.00	100.0	100.0	0.00	100.0	100.0	0.00	100.0	100.0	0.00	100.0	100.0	0.00			
	25	71.1	71.0	-0.03	71.5	71.0	-0.44	70.6	71.0	0.45	69.8	71.0	1.24	69.9	71.0	1.17	72.6	71.0	-1.58	70.9	71.0	0.14			
	30	52.5	52.8	0.30	53.0	52.8	-0.15	52.3	52.8	0.58	51.3	52.8	1.55	51.1	52.8	1.71	163.1	158.5	-4.59	52.9	52.8	-0.02			
	35	40.5	40.7	0.23	41.0	40.7	-0.34	40.1	40.7	0.59	39.0	40.7	1.70	39.0	40.7	1.71	128.3	122.1	-6.19	40.7	40.7	0.01			
	40	31.8	32.2	0.36	32.4	32.2	-0.23	31.7	32.2	0.50	30.5	32.2	1.69	30.2	32.2	2.00	103.2	96.5	-6.63	32.0	32.2	0.15			
	45	25.7	26.0	0.35	26.2	26.0	-0.22	25.5	26.0	0.48	24.3	26.0	1.69	24.0	26.0	2.06	85.2	78.0	-7.17	25.9	26.0	0.06			
	50	21.0	21.4	0.41	21.6	21.4	-0.17	21.0	21.4	0.41	19.7	21.4	1.64	19.3	21.4	2.05	71.8	64.2	-7.63	21.3	21.4	0.11			
	60							29.8	31.6	1.76															
	70							21.8	23.3	1.46															
	80							16.6	17.8	1.24															
	90							25.7	27.9	2.22															
	100							20.4	22.3	1.93															
	120							20.0	22.4	2.34															
	140							19.0	21.7	2.68															
	160							17.4	20.4	2.96															
	180							12.5	15.0	2.54															

		200							10.6	13.0	2.42															
Mean					0.62			0.33			1.49			1.46			1.47			-1.38			-2.16			
SD					0.97			1.39			0.94			0.56			0.63			6.53			5.23			
Min.					-0.03			-0.44			0.00			0.00			0.00			-7.63			-18.25			
Max.					3.31			4.22			2.96			2.14			2.06			16.24			0.15			
OMP_1Nadel-8cm		5																						535.0	492.1	-42.89
		10																						238.7	231.5	-7.19
		15	142.1	143.8	1.75	140.1	143.9	3.75	142.8	143.8	1.03	143.6	143.8	0.27	143.7	143.8	0.17							145.6	143.8	-1.79
		20	100.0	100.0	0.00	100.0	100.0	0.00	100.0	100.0	0.00	100.0	100.0	0.00	100.0	100.0	0.00							100.0	100.0	0.00
		25	73.7	75.8	2.01	74.1	74.0	-0.15	73.5	75.8	2.23	73.1	74.0	0.90	72.7	73.9	1.26							73.4	74.0	0.55
		30	56.4	56.9	0.52	57.0	56.9	-0.08	56.3	56.9	0.61	55.8	56.9	1.15	55.0	56.9	1.88							56.5	56.9	0.41
		35	44.6	45.1	0.45	45.2	45.1	-0.14	44.3	45.1	0.75	43.8	45.1	1.32	42.8	45.1	2.26							44.5	45.1	0.58
		40	35.9	36.5	0.60	36.6	36.5	-0.10	35.8	36.5	0.68	35.0	36.5	1.45	34.0	36.5	2.49							35.9	36.5	0.55
		45	29.5	30.1	0.55	30.2	30.1	-0.11	29.5	30.1	0.61	28.6	30.1	1.47	27.6	30.1	2.52							29.6	30.1	0.45
		50	24.6	25.1	0.56	25.2	25.1	-0.10	24.5	25.1	0.66	23.7	25.1	1.46	22.6	25.1	2.55							24.7	25.1	0.43
Mean					0.80			0.38			0.82			1.00			1.64									-4.89
SD					0.61			1.20			0.56			0.51			0.93									12.27
Min.					0.00			-0.15			0.00			0.00			0.00									-42.89
Max.					2.01			3.75			2.23			1.47			2.55									0.58
OMP_1Nadel-12cm		5																						505.9	454.1	-51.88
		10																						226.9	219.0	-7.81
		15	138.1	139.9	1.80	135.3	139.9	4.51	138.3	139.9	1.53	139.0	139.9	0.90	140.0	139.9	-0.19							141.9	139.9	-1.99
		20	100.0	100.0	0.00	100.0	100.0	0.00	100.0	100.0	0.00	100.0	100.0	0.00	100.0	100.0	0.00							100.0	100.0	0.00
		25	75.9	76.0	0.07	76.8	76.0	-0.83	75.7	76.0	0.31	75.0	76.0	0.97	74.7	76.0	1.31							75.3	76.0	0.64
		30	59.6	60.0	0.44	60.6	60.0	-0.61	59.4	60.0	0.62	58.7	60.0	1.28	57.6	60.0	2.41							59.3	60.0	0.71
		35	48.2	48.7	0.44	49.3	48.7	-0.65	48.0	48.7	0.63	47.2	48.7	1.51	46.1	48.7	2.59							48.0	48.7	0.68
		40	39.7	40.3	0.57	40.8	40.2	-0.58	39.5	40.3	0.72	38.6	40.3	1.65	37.4	40.2	2.87							39.6	40.2	0.68
		45	33.3	33.8	0.46	34.3	33.8	-0.53	33.1	33.8	0.72	32.1	33.8	1.68	30.9	33.8	2.88							33.2	33.8	0.60
		50	28.2	28.7	0.54	29.3	28.7	-0.54	28.1	28.7	0.66	27.1	28.7	1.63	25.8	28.7	2.98							28.2	28.7	0.51
Mean					0.54			0.10			0.65			1.20			1.86									-5.79
SD					0.49			1.59			0.38			0.51			1.16									14.84
Min.					0.00			-0.83			0.00			0.00			-0.19									-51.88
Max.					1.80			4.51			1.53			1.68			2.98									0.71
Over all measured values	Mean				**0.65**			**0.10**			**0.85**			**1.42**			**1.28**			**-0.22**			**-1.86**			**-4.82**
	SD				**0.87**			**1.25**			**0.88**			**2.25**			**1.01**			**4.88**			**4.98**			**13.09**
	Min.				**-0.43**			**-1.78**			**-0.83**			**0.00**			**-0.66**			**-7.63**			**-18.25**			**-51.88**
	Max.				**3.31**			**4.51**			**2.96**			**15.99**			**2.98**			**16.24**			**0.46**			**0.71**

Summary 5 needles in triangular configuration in the water phantom

OMP = Oncentra Masterplan
MS = Measurement series

Treatment plan		Ion chamber						
OMP Plan	see Table	Manufacturer	iba	iba	iba	iba	iba	PTW
TCC Plan	Nadel PTW HDR	Model	CC04	CC13	CC25	RAZOR[Chamber]	RAZOR[Nano Chamber]	microDiamond
Phantom	PTW water Phantom	SN	16286	16296	16125	16294	16233	123497
Source calibration data		Electrometer						
Date	02.03.2021	Manufacturer	iba	iba	iba	iba	iba	iba
Aktivity [Ci]	12.48	Model	Dose²	Dose²	Dose²	Dose²	Dose²	Dose²
SN	NLF01D85E6191	SN	00298	00298	00298	00298	00298	00298

OMP	A-Axis coordinates [mm]	C-Axis coordinates [mm]	MS correction with p_{TP} [Gy]	Planning [Gy]	Deviation [%]	MS correction with p_{TP} [Gy]	Planning [Gy]	Deviation [%]	MS correction with p_{TP} [Gy]	Planning [Gy]	Deviation [%]	MS correction with p_{TP} [Gy]	Planning [Gy]	Deviation [%]	MS correction with p_{TP} [Gy]	Planning [Gy]	Deviation [%]	MS correction with p_{TP} [Gy]	Planning [Gy]	Deviation [%]
OMP_5Nadel-3cm TD	5	0																9.215	8.200	12.37
	10	0																4.947	4.572	8.21
	15	0	6.316	6.276	0.64	2.273	2.421	-6.08	6.316	6.335	-0.31	6.09	5.92	2.89	6.315	6.217	1.58	3.251	3.056	6.38
	20	0	4.569	4.482	1.94	1.651	1.713	-3.63	4.579	4.524	1.22	4.34	4.23	2.62	4.525	4.440	1.92	2.310	2.183	5.83
	25	0	3.403	3.337	2.00	1.231	1.265	-2.74	3.406	3.368	1.11	3.21	3.15	1.87	3.326	3.305	0.62	1.713	1.625	5.41
	30	0	2.607	2.565	1.63	0.943	0.966	-2.40	2.617	2.589	1.07	2.45	2.42	1.24	2.513	2.541	-1.09	1.315	1.249	5.28
	35	0	2.052	2.024	1.43	0.744	0.758	-1.74	2.069	2.043	1.31	1.92	1.91	0.52	1.953	2.005	-2.57	1.034	0.986	4.97
	40	0	1.647	1.631	0.98	0.598	0.608	-1.60	1.661	1.647	0.87	1.54	1.54	-0.28	1.546	1.616	-4.36	0.833	0.795	4.79
	45	0	1.350	1.339	0.80	0.492	0.496	-0.97	1.365	1.352	0.94	1.25	1.26	-1.08	1.249	1.327	-5.87	0.683	0.652	4.68
	50	0	1.122	1.117	0.46	0.409	0.412	-0.78	1.135	1.127	0.73	1.03	1.05	-2.35	1.019	1.106	-7.85	0.569	0.544	4.59
	60	0	1.049	1.070	-1.97															
	70	0	0.779	0.803	-2.92															
	80	0	1.190	1.241	-4.16															
	90	0	0.931	0.982	-5.20															
	100	0	0.741	0.791	-6.36															
	120	0	0.814	0.893	-8.84															
	140	0	0.558	0.630	-11.39															
	160	0	0.629	0.732	-14.04															
	180	0	0.449	0.543	-17.23															
	200	0	0.328	0.409	-19.64															
Mean					-4.55			-2.49			0.87			0.68			-2.20			6.25
SD					6.78			1.61			0.48			1.72			3.37			2.28
Min.					-19.64			-6.08			-0.31			-2.35			-7.85			4.59
Max.					2.00			-0.78			1.31			2.89			1.92			12.37
OMP_5Nadel-3cm	5	8																6.940	6.735	3.05
	10	8																4.626	4.384	5.51
	15	8				2.114	2.286	-7.52	4.381	4.448	-1.49							3.157	2.998	5.28
	20	8				1.522	1.633	-6.76	3.199	3.200	-0.02							2.256	2.151	4.87
	25	8				1.162	1.213	-4.17	2.394	2.392	0.12							1.681	1.604	4.82
	30	8				0.898	0.930	-3.45	1.852	1.846	0.35							1.292	1.235	4.59
	35	8				0.713	0.733	-2.71										1.019	0.976	4.43
	40	8				0.576	0.590	-2.32										0.822	0.788	4.39
	45	8				0.475	0.484	-1.85										0.675	0.647	4.27
	50	8				0.397	0.403	-1.58	0.813	0.813	-0.06							0.563	0.540	4.31
Mean								-3.80			-0.22									4.55
SD								2.09			0.65									0.64
Min.								-7.52			-1.49									3.05
Max.								-1.58			0.35									5.51
OMP_5Nadel-3cm	5	16																7.803	7.262	7.44
	10	16																4.099	3.898	5.17
	15	16				2.098	2.296	-8.65	3.864	3.950	-2.18							2.708	2.597	4.28
	20	16				1.562	1.659	-5.88	2.843	2.854	-0.37							1.947	1.876	3.77
	25	16				1.203	1.256	-4.21	2.156	2.161	-0.20							1.472	1.420	3.67
	30	16				0.944	0.982	-3.91	1.687	1.689	-0.15							1.151	1.110	3.64
	35	16				0.764	0.787	-2.88										0.921	0.890	3.49
	40	16				0.626	0.643	-2.68										0.754	0.727	3.66
	45	16				0.523	0.534	-2.10										0.626	0.604	3.71
	50	16				0.442	0.450	-1.75	0.772	0.774	-0.22							0.527	0.508	3.67
Mean								-4.01			-0.62									4.25
SD								2.15			0.78									1.16
Min.								-8.65			-2.18									3.49
Max.								-1.75			-0.15									7.44

OMP_5Nadel-3cm		5	24																3.751	3.684	1.83
		10	24																2.760	2.692	2.51
		15	24				1.615	1.758	-8.15	2.966	3.025	-1.94							2.039	1.988	2.58
		20	24				1.268	1.343	-5.59	2.294	2.310	-0.69							1.558	1.518	2.61
		25	24				1.011	1.055	-4.19	1.807	1.816	-0.45							1.228	1.193	2.94
		30	24				0.817	0.849	-3.75	1.456	1.460	-0.32							0.991	0.960	3.23
		35	24				0.676	0.695	-2.84										0.811	0.786	3.16
		40	24				0.563	0.578	-2.63										0.673	0.654	2.88
		45	24				0.476	0.487	-2.24										0.568	0.551	3.19
		50	24				0.407	0.415	-1.90	0.710	0.714	-0.48							0.484	0.469	3.09
Mean									-3.91			-0.78									2.80
SD									1.95			0.59									0.41
Min.									-8.15			-1.94									1.83
Max.									-1.90			-0.32									3.23
Over all measured values	Mean					**-4.55**			**-3.55**			**-0.05**			**0.68**			**-2.20**			**4.46**
	SD					**6.78**			**2.06**			**0.93**			**1.72**			**3.37**			**1.81**
	Min.					**-19.64**			**-8.65**			**-2.18**			**-2.35**			**-7.85**			**1.83**
	Max.					**2.00**			**-0.78**			**1.31**			**2.89**			**1.92**			**12.37**

	Date	[]	15.04.2021	07.04.2021	14.04.2021	21.04.2021	16.04.2021	25.03.2021
Plan	Source aktivity	[Ci]	8.26	8.90	8.33	7.80	8.18	10.06
	Total traeatment time	[s]	2800	4032	11200	2800	2800	2880
	Method	[]	Timed continuous	Timed continuous	Timed continuous	Timed continuous	Timed continuous	Timed continuous
	Range	[]	Low	Low	Low	Low	Low	Low
	Length	[mm]	see Table	see Table	see Table	see Table	see Table	see Table
	Air pressure	[hPa]	1002.4	993.8	1003.8	993.8	1001.3	1001.4
	Temperature	[°C]	21.3	22.3	21.8	21.6	21.3	22.5
	P_{TP}	[]	1.02	1.03	1.02	1.02	1.02	1.02

				CC04			CC13			CC25			RAZOR[Chamber]			RAZOR[Nano Chamber]			microDiamond		
OMP		A-Axis coordinates [mm]	C-Axis coordinates [mm]	Normalised whit 20 mm [Gy]	Planning [Gy]	Deviation of normalised data [%]	Normalised whit 20 mm [Gy]	Planning [Gy]	Deviation of normalised data [%]	MS correction with P_{TP} [Gy]	Planning [Gy]	Deviation of normalised data [%]	Normalised whit 20 mm [Gy]	Planning [Gy]	Deviation of normalised data [%]	Normalised whit 20 mm [Gy]	Planning [Gy]	Deviation of normalised data [%]	Normalised whit 20 mm [Gy]	Planning [Gy]	Deviation of normalised data [%]
OMP_5Nadel-3cm	TD	5	0																398.9	375.7	-23.24
		10	0																214.2	209.5	-4.71
		15	0	138.2	140.0	1.80	137.7	141.3	3.60	137.9	140.0	2.12	140.4	140.0	-0.37	139.6	140.0	0.46	140.8	140.0	-0.73
		20	0	100.0	100.0	0.00	100.0	100.0	0.00	100.0	100.0	0.00	100.0	100.0	0.00	100.0	100.0	0.00	100.0	100.0	0.00
		25	0	74.5	74.4	-0.05	74.5	73.9	-0.68	74.4	74.4	0.08	73.9	74.5	0.54	73.5	74.4	0.95	74.2	74.5	0.29
		30	0	57.1	57.2	0.17	57.1	56.4	-0.72	57.1	57.2	0.09	56.5	57.2	0.77	55.5	57.2	1.69	56.9	57.2	0.30
		35	0	44.9	45.2	0.23	45.1	44.2	-0.87	45.2	45.2	-0.04	44.2	45.1	0.92	43.2	45.2	1.99	44.8	45.2	0.36
		40	0	36.1	36.4	0.34	36.2	35.5	-0.75	36.3	36.4	0.13	35.4	36.4	1.03	34.2	36.4	2.24	36.0	36.4	0.35
		45	0	29.5	29.9	0.33	29.8	29.0	-0.80	29.8	29.9	0.08	28.8	29.9	1.08	27.6	29.9	2.28	29.6	29.9	0.32
		50	0	24.6	24.9	0.36	24.8	24.0	-0.71	24.8	24.9	0.12	23.7	24.9	1.21	22.5	24.9	2.39	24.6	24.9	0.29
		60	0	23.0	23.9	0.92															
		70	0	17.1	17.9	0.85															
		80	0	26.0	27.7	1.66															
		90	0	20.4	21.9	1.54															
		100	0	16.2	17.7	1.44															
		120	0	17.8	19.9	2.11															
		140	0	12.2	14.0	1.84															
		160	0	13.8	16.3	2.56															
		180	0	9.8	12.1	2.28															
		200	0	7.2	9.1	1.93															
Mean						1.13			-0.12			0.32			0.65			1.50			-2.68
SD						0.84			1.43			0.68			0.52			0.86			7.01
Min.						-0.05			-0.87			-0.04			-0.37			0.00			-23.24
Max.						2.56			3.60			2.12			1.21			2.39			0.36
OMP_5Nadel-3cm		5	8																307.7	313.1	5.42
		10	8																205.1	203.8	-1.25
		15	8				138.9	140.0	1.14	136.9	139.0	2.05							139.9	139.4	-0.55
		20	8				100.0	100.0	0.00	100.0	100.0	0.00							100.0	100.0	0.00
		25	8				76.3	74.3	-2.06	74.8	74.7	-0.10							74.5	74.6	0.03
		30	8				59.0	57.0	-2.02	57.9	57.7	-0.21							57.3	57.4	0.15
		35	8				46.8	44.9	-1.95										45.2	45.4	0.19
		40	8				37.9	36.1	-1.72										36.4	36.6	0.17
		45	8				31.2	29.6	-1.56										29.9	30.1	0.17
		50	8				26.0	24.7	-1.37	25.4	25.4	0.01							25.0	25.1	0.13
Mean									-1.19			0.35									0.45
SD									1.08			0.85									1.71
Min.									-2.06			-0.21									-1.25
Max.									1.14			2.05									5.42

OMP_5Nadel-3cm		5	16																400.8	387.1	-13.70
		10	16																210.6	207.8	-2.81
		15	16				134.3	138.4	4.07	135.9	138.4	2.52							139.1	138.4	-0.68
		20	16				100.0	100.0	0.00	100.0	100.0	0.00							100.0	100.0	0.00
		25	16				77.0	75.7	-1.34	75.8	75.7	-0.13							75.6	75.7	0.07
		30	16				60.4	59.2	-1.24	59.3	59.2	-0.13							59.1	59.2	0.07
		35	16				49.0	47.4	-1.51										47.3	47.4	0.13
		40	16				40.1	38.8	-1.32										38.7	38.8	0.04
		45	16				33.5	32.2	-1.29										32.2	32.2	0.02
		50	16				28.3	27.1	-1.19	27.1	27.1	-0.04							27.1	27.1	0.03
Mean									-0.48			0.44									-1.68
SD									1.77			1.04									4.09
Min.									-1.51			-0.13									-13.70
Max.									4.07			2.52									0.13
OMP_5Nadel-3cm		5	24																240.8	242.6	1.83
		10	24																177.1	177.3	0.17
		15	24				127.4	130.9	3.55	129.3	130.9	1.65							130.9	130.9	0.03
		20	24				100.0	100.0	0.00	100.0	100.0	0.00							100.0	100.0	0.00
		25	24				79.8	78.6	-1.17	78.8	78.6	-0.19							78.8	78.6	-0.25
		30	24				64.4	63.2	-1.23	63.5	63.2	-0.23							63.6	63.2	-0.39
		35	24				53.3	51.8	-1.51										52.1	51.8	-0.28
		40	24				44.4	43.1	-1.35										43.2	43.1	-0.11
		45	24				37.6	36.3	-1.29										36.5	36.3	-0.21
		50	24				32.1	30.9	-1.21	31.0	30.9	-0.07							31.0	30.9	-0.14
Mean									-0.53			0.23									0.06
SD									1.60			0.71									0.61
Min.									-1.51			-0.23									-0.39
Max.									3.55			1.65									1.83
Over all measured values	Mean					**1.13**			**-0.58**			**0.33**			**0.65**			**1.50**			**-0.96**
	SD					**0.84**			**1.54**			**0.82**			**0.52**			**0.86**			**4.35**
	Min.					**-0.05**			**-2.06**			**-0.23**			**-0.37**			**0.00**			**-23.24**
	Max.					**2.56**			**4.07**			**2.52**			**1.21**			**2.39**			**5.42**